SAPIENZA
UNIVERSITÀ DI ROMA

Sapienza University of Rome

Graduate School: Biology and Molecular Medicine

Department: Molecular Medicine

PhD: Immunological, Haematological and Rheumatological Sciences

Curriculum: Immunology and Immunopathology

XXIX cycle

Maltonis: a modulator of chromatin structure as potential anti-cancer drug

Coordinator: Prof. Angela Santoni

Tutor:

Prof. Angela Santoni

Co-tutor:

Prof. Mirco Fanelli

PhD candidate:

Alfredo Errico Provenzano

TABLE OF CONTENTS

ABSTRACT

Hydroxypyrones comprise several classes of molecules characterised by high synthetic versatility and interesting pharmaceutical activities. Recently, with the aim to produce innovative anti-cancer agents, we developed a new class of compounds based on the 3-hydroxy-2-methyl-4-pyrone unit (maltol). In this study, we analysed a previous selected molecule referred to as maltonis, in order to assess its anti-proliferative activity both *in vitro* and *in vivo* and to characterize its mechanism of action.

We firstly tested *in vitro* anti-tumour efficacy on a wide panel of human tumour cell lines of different origins, subsequently focusing on hematopoietic cancer cell lines that resulted among the most sensitive to maltonis treatments.

Maltonis exposure led to a dose-dependent reduction in cell survival in the leukaemia cell models studied. Sublethal concentrations of maltonis induced profound cell cycle perturbations, particularly affecting G2-M phase, whereas treatments with lethal doses caused the induction of programmed cell death.

In order to clarify the mechanism of action, we showed by cell-free assays that maltonis is able to alter the chromatin structure inducing the formation of covalent bonds between genomic DNA and proteins. In addition, we demonstrated the activation of DNA damage response as a consequence of maltonis treatments.

Moreover, a microarray-based comparative analysis allowed us to better define the molecular response triggered by maltonis in HL-60 cells, and to identify a peculiar distribution of down-regulated genes related to specific genomic features.

Finally, a pilot *in vivo* experiment on a human AML (HL-60) xenograft murine model demonstrated the tolerability and efficacy of maltonis that allowed to slightly increase mice survival time.

Overall, these results show that maltonis exerts its anti-proliferative activity through the induction of complex chromatin structural modifications, thus affecting key cellular processes such as RNA processing and DNA replication.

ABBREVIATIONS

AML	Acute myeloid leukaemia
bp	Base pair
DAVID	Database for Annotation, Visualization and Integrated Discovery
DDR	DNA damage response
DR	Down-regulated genes
FA	Formaldehyde
G4	G-quadruplex
GI	Growth inhibition
GO	Gene Ontology
IC_{50}	Half maximal inhibitory concentration
kb	Kilobase
NCI	National Cancer Institute
PCA	Principal Component Analysis
PQS	Putative G-quadruplex sequence
RT	Room temperature
SD	Standard deviation
SDS	Sodium dodecyl sulfate
TCA	Trichloroacetic acid
TSS	Transcription Start Site
UR	Up-regulated genes

INTRODUCTION

New molecules for potential pharmacological uses are continuously synthesized, developed, and tested. Anti-neoplastic agents are one of the main targets because, although great progress has been made in the treatment of neoplastic diseases, the survival of patients affected by tumour remains in many cases very limited (Tobias and Hochhauser, 2010). In these cases, the main problems are related to the lack of specific therapies as well as to the resistance to currently used chemotherapeutic drugs, which are furthermore cytotoxic, thus causing severe side effects. In this light, there is an urgent necessity to identify and synthesize new molecules showing both a higher effective and/or selective anti-tumour activity and increased human body tolerability.

Moreover, a detailed comprehension of drug molecular mechanisms could help scientists to understand the basic science involved and, therefore, to develop new and improved drugs with fewer side effects.

The aims of our studies were to assess the anti-proliferative effects of maltonis, a maltol derived compound, both *in vitro* and *in vivo* and to characterize its mechanism of action.

In this chapter we will provide fundamental concepts related to cancer, hydroxypyrones, the family of molecules maltonis belongs to, and chromatin landscape, in order to proper illustrate Results and Discussion sections.

1. Cancer

Cancer is one of the main causes of morbidity and mortality worldwide, with approximately 14.1 million new cases and 8.2 million cancer related deaths reported in 2012, thus affecting life expectancy and producing a negative impact on society (Ferlay et al, 2015). World Health Organization (WHO) estimates that if current cancer rates remain unchanged the number of new cases is expected to rise by about 75%. This will bring the number of cancer cases close to 25 million over the next two decades (Stewart and Wild, 2016).

1.1 The hallmarks of cancer

Cancer is a complex progressive multistep disorder that results from the accumulation of genetic and epigenetic abnormalities, which lead to the transformation of normal cells into malignant derivatives. Thus, cancer risk increases with age, because more time for the accumulation of initiating mutations has elapsed and the effects of molecular repair mechanisms are reduced. Largely, these changes are the result of the interaction between intrinsic genetic factors and three categories of external agents, including:

- physical carcinogens, such as ultraviolet and ionizing radiation;
- chemical carcinogens, such as asbestos, components of tobacco smoke, aflatoxins (food contaminants) and arsenic (a drinking water contaminant); and
- biological carcinogens, such as infections from certain viruses, bacteria or parasites (Elliot and Elliot, 2009).

Cancer cells can acquire distinctive and complementary capabilities that enable tumour growth and metastatic dissemination, providing them with a competitive advantage over normal cells (Hanahan and Weinberg, 2000):

- *self-sufficiency in growth signals*: tumour cells generate many of their own growth signals, thereby reducing their dependence on stimulation from their normal tissue microenvironment. This liberation from dependence on exogenously derived signals disrupts a critically important homeostatic mechanism that normally operates to ensure a proper behaviour of the various cell types within a tissue.
- *insensitivity to growth-inhibitory (anti-growth) signals*: cancer cells are also able to circumvent powerful programs that negatively regulate cell proliferation; many of these programs depend on the actions of tumour suppressor genes (*e.g. RB1*).
- *evasion of programmed cell death*: tumour cells gain the ability to limit or circumvent apoptosis through a variety of strategies such as the loss of p53 tumour suppressor function, the increased expression of anti-apoptotic regulators (Bcl-2, Bcl-xL) or of survival signals (Igf1/2) and the down-regulation of pro-apoptotic factors (Bax, Bim).
- *limitless replicative potential*: tumours acquire the proficiency to maintain telomeric DNA at lengths sufficient to avoid triggering senescence or apoptosis by up-regulating expression of telomerase or, less frequently, via an alternative recombination-based telomere maintenance mechanism.
- *sustained angiogenesis*: tumours require sustenance in the form of nutrients and oxygen as well as an ability to evacuate metabolic wastes and carbon dioxide. Tumours appear to activate the "angiogenic switch" by changing the balance of angiogenesis inducers (*e.g.* vascular endothelial growth factor A) and countervailing inhibitors (*e.g.* thrombospondin-1).
- *tissue invasion and metastasis*: the capability for invasion and metastasis enables cancer cells to escape the primary tumour mass and colonize new terrain in the body. The multistep process of invasion and metastasis involves several cell-biological traits

including loss of adherens junctions, expression of matrix-degrading enzymes, increased motility, and heightened resistance to apoptosis (Figure I).

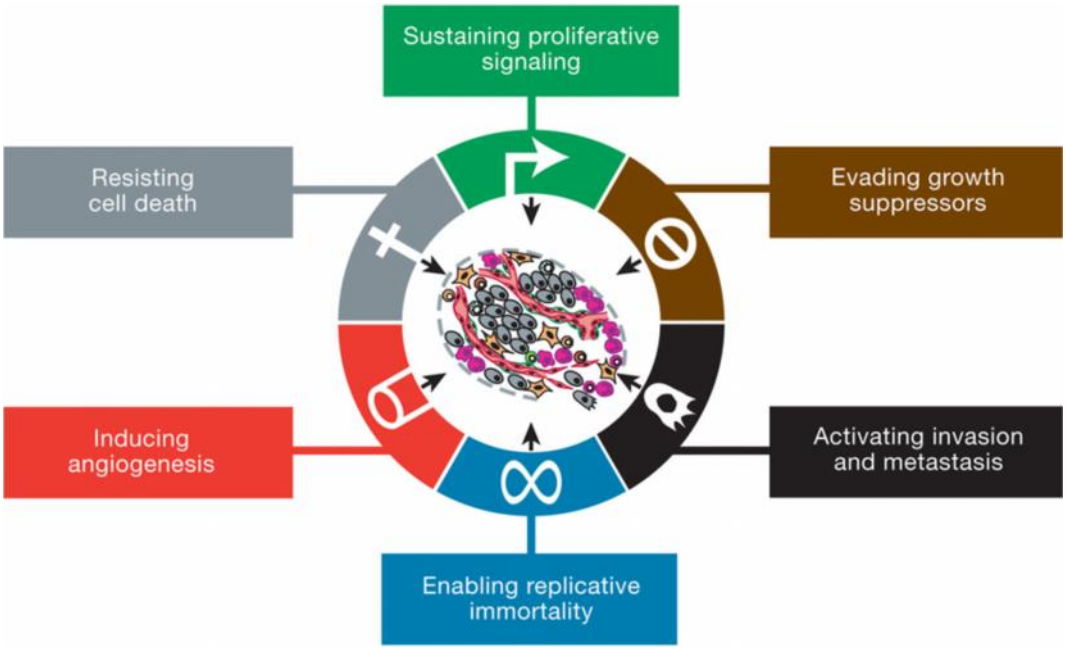

Figure I. Schematic representation of the six biological capabilities of cancer cells acquired during their development.

(Adapted from Hanahan and Weinberg, 2011)

Their acquisition is made possible by two enabling characteristics (Figure II). In fact, underlying these hallmarks are genome instability, which generates the genetic diversity that expedites their acquisition, and inflammation, which fosters multiple hallmark functions (Hanahan and Weinberg, 2011).

Yet other distinct attributes of cancer cells have been proposed to be functionally important (Colotta et al, 2009; Negrini et al, 2010), two such attributes are particularly compelling. The first involves major reprogramming of cellular energy metabolism in order to support continuous cell growth and proliferation while the second concerns the active evasion by cancer cells from attack and elimination by immune cells. Both of these capabilities may

well prove to facilitate the development and progression of many forms of human cancer and therefore can be considered to be emerging hallmarks of cancer (Figure II).

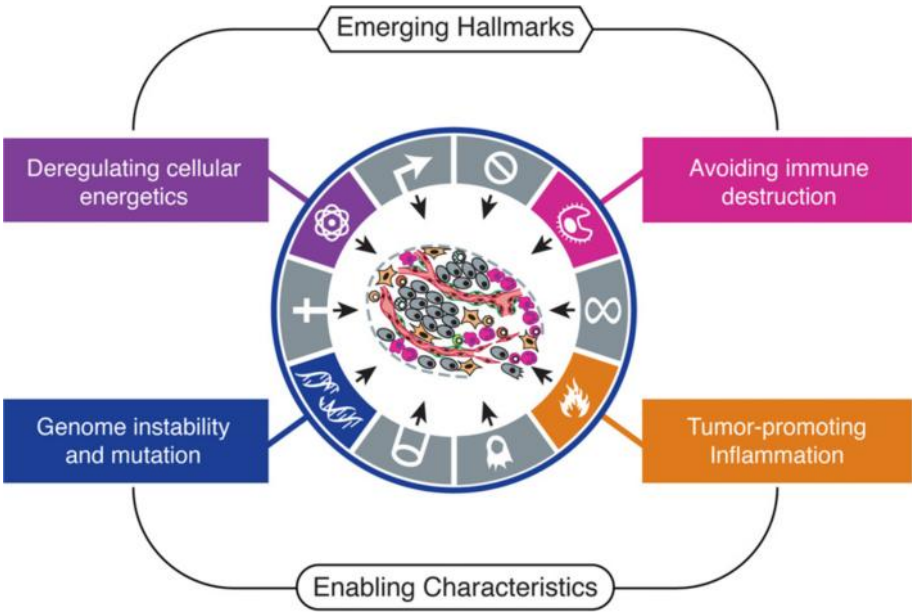

Figure II. Schematic representation of emerging hallmarks and enabling characteristics involved in the pathogenesis of cancers.

(Adapted from Hanahan and Weinberg, 2011)

1.2 Cancer therapy

Due to the multitude of different cancer types, there are several treatment options, depending upon the location and stage of the cancer and the patient's general health state.

To date, surgery, radiotherapy and systemic chemotherapy still comprise the standard treatment in a majority of proliferative disease, showing over many decades to be highly effective in extending the survival of cancer patients and in eradicating certain types of tumours with curative outcomes (Weinberg, 2014).

In particular, there are several classes of chemotherapeutics, which can be distinguished by their structures and mechanisms of action (Haskell, 2001):

- alkylating agents: impair cell functions by alkylation of DNA, RNA and proteins, thus inhibiting cell replication. Examples are triazines, nitrogen mustards, alkyl sulfonates and nitrosoureas.
- metal-based drugs: depending on their structure, there are numerous different mechanisms of action. An important example is represented by the class of platinum-containing drugs, which includes cisplatin, carboplatin and oxaliplatin. These platinum complexes react in the body, binding to DNA and causing DNA strands cross-linking, which ultimately triggers cell death (Fanelli et al, 2016).
- antimetabolites: compete with or substitute biomolecules involved in DNA and RNA synthesis thus altering the critical pathways of nucleotide synthesis. Examples are folic acid, purine and pyrimidine analogues (*e.g.* 5-fluorouracil).
- topoisomerase inhibitors: topoisomerases are essential enzymes that maintain the topology and integrity of DNA. Inhibition of topoisomerase interferes with all central DNA processing steps such as replication, transcription and recombination (*e.g.* topotecan and etoposide).

Newer approaches for cancer treatment include anti-tumour antibiotics, hormone inhibitors, mitosis inhibitors, monoclonal antibodies, signal transduction and enzyme inhibitors.

The current challenge is to develop novel therapeutic paradigms exploiting the knowledge derived from molecular, cellular and systems biology studies of tumour formation and progression (Pavet et al, 2011).

Despite the pleiotropic nature of tumours, several characteristics are shared by almost all malignancies; therefore a plethora of therapeutic approaches targeting the corresponding pathways/key players that support or are essential for tumour development are being

explored and tested (Figure III) (Ferrara et al, 2004; Tennant et al, 2010; Hanahan and Weinberg, 2011).

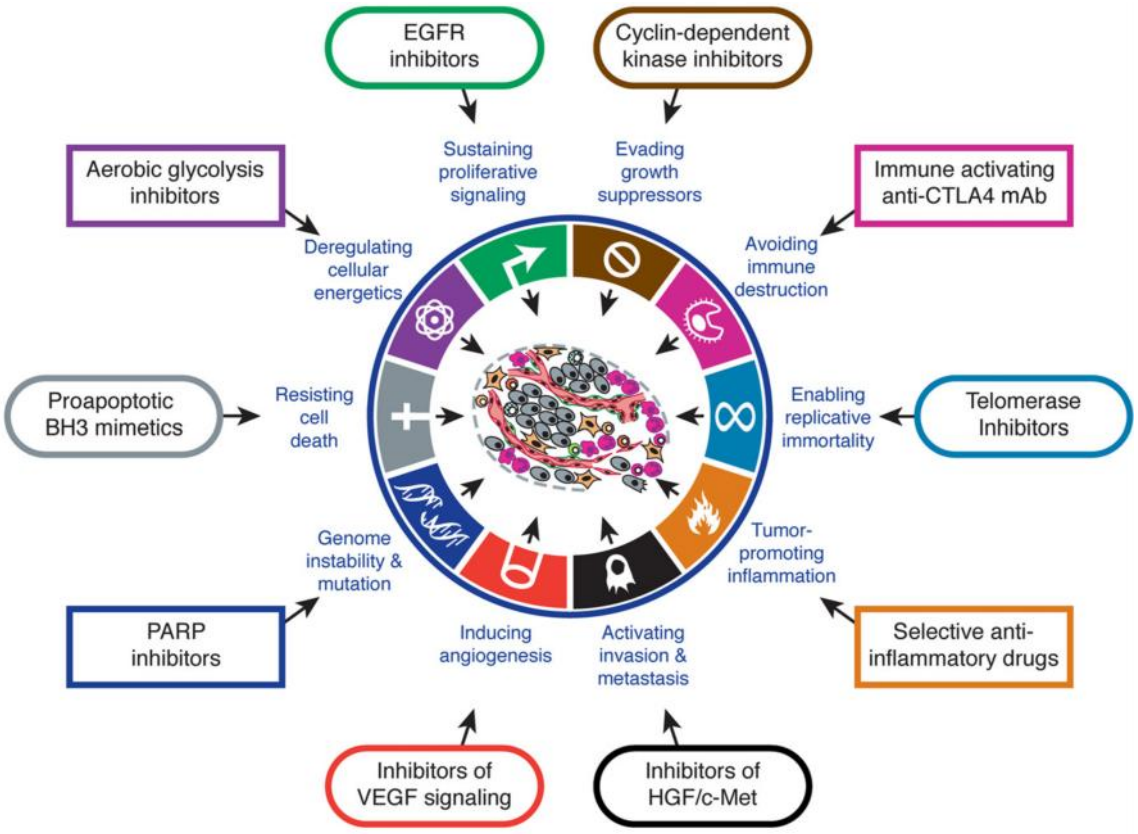

Figure III. Therapeutic targeting of the hallmarks of cancer. Illustrative examples of drugs that interfere with each of the acquired capabilities necessary for tumour growth and progression.

(Adapted from Hanahan and Weinberg, 2011)

Furthermore, abnormal function/recruitment of histone-epigenetic modulators is also recognized to have a role in tumorigenesis (Feinberg and Tycko, 2004; Esteller, 2008). Consequently, epigenetic enzymes have been identified as valuable drug targets, as aberrant DNA methylation and histone modifications can be reverted by the administration of epigenetic drugs referred to as epi-drugs.

Moreover, although chemotherapy has advanced into the era of targeted drugs, the anti-tumour efficacies of current therapies are limited, most likely because of the high degree of cancer clonal heterogeneity, intra-tumour genetic heterogeneity and cell signal complexity.

As shutdown of a single target does not necessarily eradicate the cancer, the use of combinations of different drugs has been proposed, and some pioneering research has been conducted to examine the efficacy of this strategy (Li et al, 2014). Combination therapy allows for dose reduction at similar efficacy, due to synergistic action and its effect through different therapeutic targets can minimize the risk of resistance development (Pavet et al, 2011).

1.3 Haematological malignancies

Among the over 400 types of cancer, a broad group is represented by haematological neoplasms affecting the blood, bone marrow and lymphoid system.

Hematopoietic malignancies comprise acute and chronic leukaemias, lymphomas, myeloproliferative disorders, and myelodysplastic syndromes.

The current approach to the classification of haematopoietic and lymphoid malignancies is based on the integration of morphological, phenotypic, genetic, and clinical features, which allows the identification of distinct disease entities (Swerdlow et al, 2008).

In particular, leukaemias are defined by an expansion of immature white blood cells in the bone marrow and blood, where a lack of mature blood cells together with a suppression of normal residual haematopoiesis eventually leads to anaemia, thrombocytopenia, and leukopenia, which result in fatigue, bleeding, and infections.

Molecularly, leukaemias represent a heterogeneous disorder characterized by different rearrangements and dysregulations of genes with important functions in cellular growth, differentiation, and death (Cline, 1994).

In 2012, there were almost 352000 new cases of leukaemia worldwide, and about 265000 deaths. The disease ranks as the 11th most frequent in terms of cancer incidence and the 10th most common cause of cancer death (Stewart and Wild, 2016).

Leukaemias can be divided into two main categories, acute and chronic, depending on the level of maturation of the cells involved and their rates of progression:

- *Acute* leukaemias are characterized by a rapid increase in the number of immature blood cells (called blasts). Leukaemia cells multiply quickly and don't carry out their normal functions. Acute leukaemias required an aggressive and timely treatment in order to avoid accumulation of the malignant cells and their spreading to other organs of the body.
- *Chronic* leukaemias are characterized by the excessive build-up of relatively mature, but still abnormal, white blood cells. Typically, chronic leukaemias tend to progress over a long period of time. Whereas acute leukaemias must be treated immediately, chronic forms are often monitored for some time before treatment to ensure maximum effectiveness of therapy.

Additionally, leukaemias are also classified according to the type of bone marrow cell that is affected:

- *Myeloid* leukaemias start in immature forms of myeloid cells: white blood cells (other than lymphocytes), red blood cells, or platelet-making cells (megakaryocytes). They are also known as *myelocytic*, *myelogenous*, or *non-lymphocytic* leukaemias.
- *Lymphocytic* leukaemias start in immature forms of lymphocytes. They are also known as *lymphoid* or *lymphoblastic* leukaemias.

By considering whether leukaemias are acute or chronic and whether they are myeloid or lymphocytic, they can be divided into 4 main types:

- Acute myeloid leukaemia (AML);
- Chronic myeloid leukaemia (CML);
- Acute lymphocytic leukaemia (ALL);
- Chronic lymphocytic leukaemia (CLL).

In particular, acute myeloid leukaemia, also known as acute myelogenous leukaemia or acute non-lymphoblastic leukaemia, is a heterogeneous disease characterized by increased blasts (usually ≥ 20% myeloblasts, monoblasts plus promonocytes, and/or megakaryoblasts) in blood or bone marrow.

In recent years, there has been improvement in survival, particularly in younger people, but AML remains a fatal disease for most patients. The WHO classification of AML assigns patients to categories useful for predicting outcome. Some are classified according to genetic abnormalities that determine morphological and clinical features (AML with recurrent genetic abnormalities), others have morphology and/or genetics that relate them to myelodysplastic syndromes (AML with myelodysplasia-related changes), some are unique because they follow prior cytotoxic therapy (Therapy-related myeloid neoplasms), and the remainder are classified by lineage involvement and degree of differentiation (Arber et al, 2016).

Currently, karyotype and age are the most powerful predictors of prognosis (Burnett, 2012; Grimwade, 2012). Whole-genome and exome sequencing have revealed a plethora of gene mutations and submicroscopic genetic defects in this type of leukaemia. Although the prognostic significance of some alterations, particularly mutated *FLT3*, *NPM1*, and *CEBPA*, has been recognized, the significance of many others remains to be determined (Patel et al, 2012). A separate study involving 200 cases reported that AML genomes have fewer mutations than those of most other adult cancers, with an average of only 13. A total of 23 genes were significantly mutated, and nearly all samples had at least one non-synonymous mutation in one of nine categories of genes relevant for pathogenesis, including transcription factor fusions (18% of cases), the gene encoding nucleophosmin (*NPM1*) (27%), tumour suppressor genes (16%), DNA methylation-related genes (44%), signalling genes (59%), chromatin modifying genes (30%), myeloid transcription factor

genes (22%), cohesin-complex genes (13%), and spliceosome-complex genes (14%) (TCGA Research Network, 2013).

2. The family of hydroxypyrones

Hydroxypyrones comprise several classes of molecules characterised by high synthetic versatility and high affinity for a range of metal ions, rendering these ligands excellent choices for the formulation of therapeutic and/or diagnostic metallopharmaceuticals.

Structurally, hydroxypyrones are heterocycles with an hydroxyl group *ortho* to a ketone, providing two oxygen donor groups in close proximity (Figure IV) (Santos, 2002).

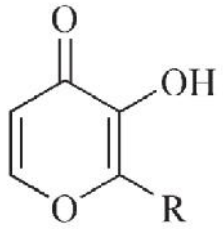

Figure IV. Chemical structure of 3-hydroxy-4-pyrones.

The main feature of hydroxypyrones is the ability to form exceptionally stable and, in many cases, neutrally charged complexes with a wide variety of metal ions, including the trivalent cations Fe^{3+}, Al^{3+}, Ga^{3+} and In^{3+}, and the divalent ions Zn^{2+} and Ru^{2+} and such metal chelation capacity can be attributed to a substantial charge delocalization within the six-membered ring (Thompson et al, 2006).

Early applications of hydroxypyrones to medicinal inorganic chemistry generally fall into one of two main areas: 1) ligand development for potentiation of in situ metal-ion complex formation and subsequent removal of excess metal ion(s), or 2) metal ion-ligand complex formation for improving absorption and/or biodistribution characteristics of a particular metal ion (Thompson and Orvig, 2003).

2.1 Maltol and its derivatives

Maltol (3-hydroxy-2-methyl-4-pyrone, Figure V), one of the most studied hydroxypyrones, is a natural compound extensively used, for its flavour and antioxidant properties, as food additive to impart a desirable malty taste and odour to breads, cakes, beer and other beverages (Cavalieri, 1947).

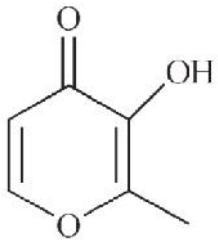

Figure V. Chemical structure of maltol, 3-hydroxy-2-methyl-4-pyrone.

Maltol, like related 3-hydroxy-4-pyrones, is an efficient chelator of metal ions such as Fe^{3+}, Ga^{3+}, Al^{3+}, and VO^{2+} (Thompson et al, 2006). Ferric maltol is used in the treatment of anaemia caused by iron deficiency (Gasche et al, 2015; Stallmach and Büning, 2015), and oxovanadium(IV) complexes of ligands based on maltol were developed as insulin enhancing agents for treatment of type-2 diabetes mellitus (Saatchi et al, 2005).

Although its high bioavailability and favourable toxicity profiles have been known for a long time, only recently maltol was found to perform anti-neoplastic activities against different cancer cellular models. Reactive oxygen species (ROS) generation and the consequent induction of DNA breaks have been hypothesised as possible mechanisms responsible for this activity (Hironishi et al, 1996; Yasumoto et al, 2004; Murakami et al, 2006). For this reason, during the last few years, several maltol-derived compounds have been synthesised and exploited in the formulation of new potential metal-based anti-tumour drugs (Jakupec and Keppler, 2004; Barve et al, 2009; Kandioller et al, 2009).

2.2 Maltonis

Recently, with the goal to produce new anticancer agents, the research group of Prof. Mirco Fanelli in collaboration with that of Prof. Vieri Fusi (Department of Pure and Applied Sciences, University of Urbino) developed a new class of maltol-derived molecules coupling maltol and polyamine symmetrically (Fanelli and Fusi, 2010).

The newly designed compounds show two [(3-hydroxy-4-pyron-2-yl)methyl]amine units separated by different aliphatic spacers with or without a cyclic skeleton (Figure VI).

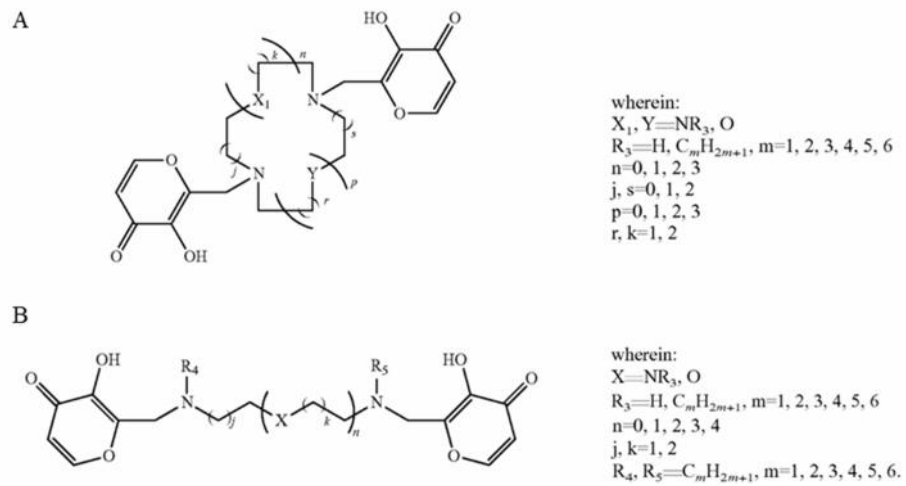

Figure VI. Chemical structure of maltol-derived compounds formed by two [(3-hydroxy-4-pyron-2-yl)methyl]amine units separated by different aliphatic spacers with (A) or without (B) a cyclic skeleton.

Malten (N,N'-bis((3-hydroxy-4-pyron-2-yl)methyl)-N,N'-dimethylethylendiamine), the first selected molecule, showed anti-proliferative activity in eight tumour cell lines derived from both haematopoietic and solid tumours. Malten exposure led to a dose dependent reduction in cell survival in all of the neoplastic models analysed, associated with the activation of programmed cell death and cell cycle arrest (Amatori et al, 2010). In accordance with biological studies, it was demonstrated that malten treatment modulates the expression of genes having key roles in cell cycle progression and apoptosis. Complex

DNA structural modifications are induced by malten, suggesting that a DNA intermolecular cross-linking activity could be part of the mechanism of action of the compound (Amatori et al, 2010).

Interestingly, the key of the activity, compared to the previous maltol derivatives reported, seems to consist in the simultaneous presence of the two amino-spaced maltols.

In light of these results, a new preliminary screening was performed among the maltol-derived compounds containing a cyclic aliphatic spacer and maltonis (4,10-bis[(3-hydroxy-4-pyron-2-yl)methyl]-1,7-dimethyl-1,4,7,10-tetraazacyclododecane) was selected.

Maltonis synthetic procedure is easy and low-cost and includes the coupling of maltol, appropriately protected and activated, with the secondary amine 1,7-dimethyl-1,4,7,10-tetraazacyclododecane (Figure VII).

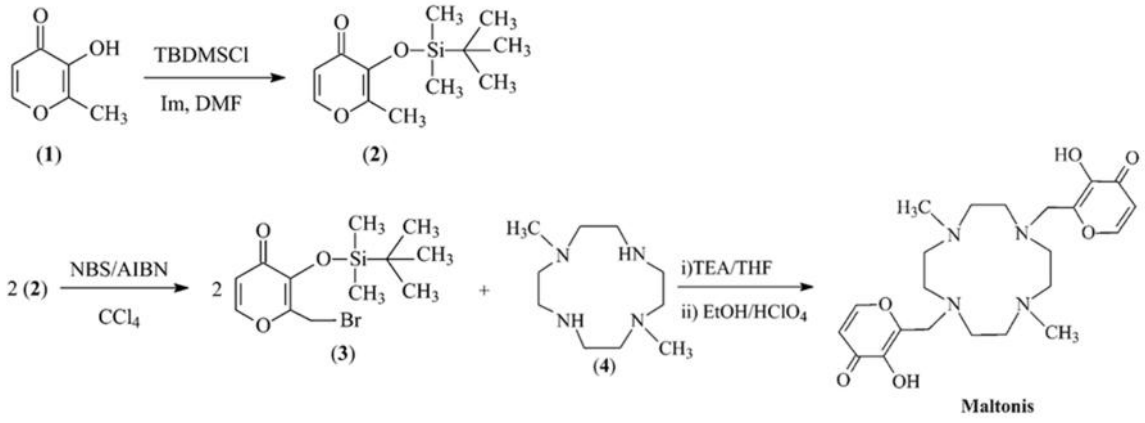

Figure VII. Synthetic pathway of maltonis. The procedure includes the coupling of maltol (1), appropriately protected (2), and activated (3) with the secondary amine 1,7-dimethyl-1,4,7,10-tetraazacyclododecane (4). TBDMSCl, tert-Butyldimethylsilyl chloride; Im, Imidazole; DMF, N,N-Dimethylformamide; NBS, N-Bromosuccinimide; AIBN, Azobisisobutyronitrile; CCl_4, Carbon tetrachloride; TEA, Triethylamine; THF, Tetrahydrofuran; EtOH, Ethanol; $HClO_4$, Perchloric acid.

(Adapted from Amatori et al, 2012)

Basicity studies showed that at pH = 7.4, the main species presents in solution for maltonis is the protonated form HL^+, with an internal charge separation (Figure VIII).

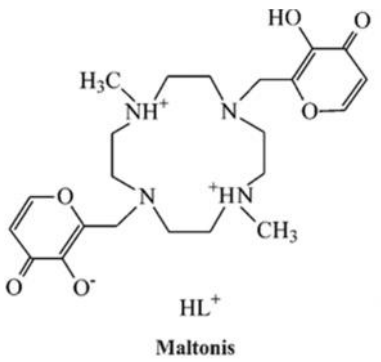

Figure VIII. Location of acidic hydrogen atoms in the protonated HL^+ species of maltonis.

(Adapted from Amatori et al, 2012)

In view of its overall positive charge, maltonis HL^+ species is likely to interact with the negatively charged DNA. A preliminary study on this possibility demonstrated that the HL^+ species of maltonis is able to bridge two double-helix fragments through H-bonding and π-interactions at 27°C in vacuo and water model. A non-covalent approach with the DNA moiety could be the first step for maltonis to place itself in a favorable position to allow the formation of covalently bound chromatin structures (Amatori et al, 2012).

Moreover, first attempts to assess anti-proliferative activity of maltonis showed that it significantly reduces sarcoma cell viability and tumour growth both *in vitro* and *in vivo* (Guerzoni et al, 2014).

3. Chromatin structure and function

Chromatin is composed by naked DNA wrapped around nucleosomes, organized structures of specialized proteins called histones, and then packed to form chromosomes (Figure IX).

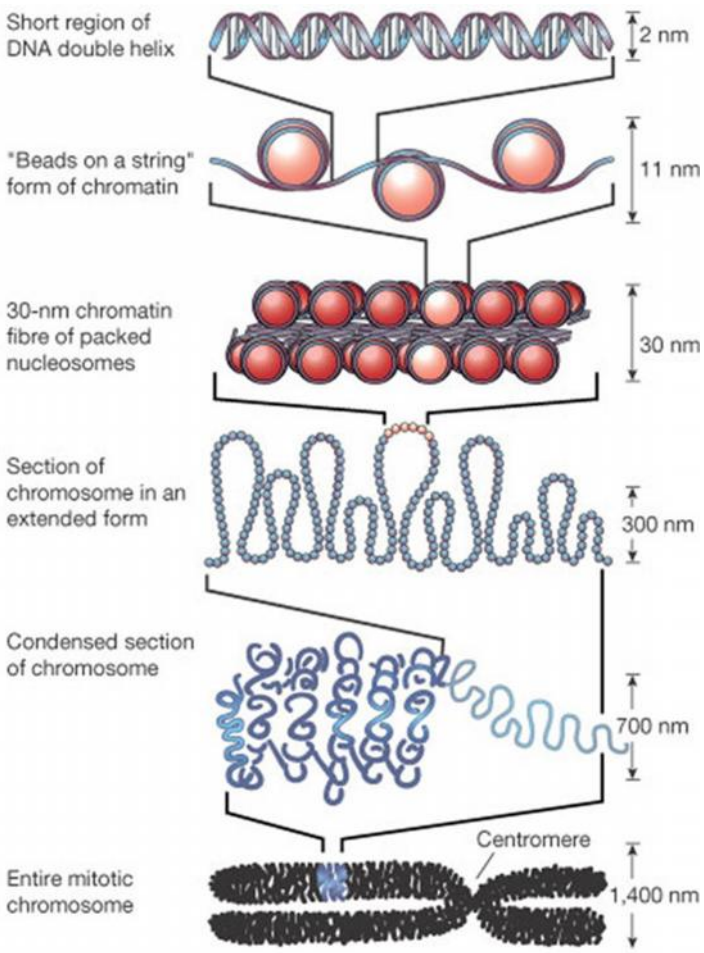

Figure IX. The organization of DNA within the chromatin structure. The lowest level of organization is the nucleosome, in which two helical turns of DNA are wound around the outside of a histone octamer. Nucleosomes are connected to one another by short stretches of linker DNA. At the next level of organization the string of nucleosomes is folded into a fibre about 30 nm in diameter, and these fibres are then further folded into higher-order structures.

(Adapted from Felsenfeld and Groudine, 2003)

Chromatin is not a mere depository of the genomic content but rather a signal transduction platform for extracellular or intracellular signals that regulates all genome functions, including gene expression, DNA replication and genome stability.

Upstream signals are translated by chromatin into either transient or long-lasting (and heritable during cell division) modifications, thereby allowing chromatin to serve the double function of adapting cells to the environment changes while maintaining their lineage and/or identity. These modifications forms the epigenome: they are not modifications of DNA sequences but chemical changes happening on DNA (DNA methylation) or on specific regions of histone proteins called tails (histone modifications) that modify chromatin structure in different conformations as more open (euchromatin) and available to be bound by other proteins, or closed, compacted and then repressed (heterochromatin) (Felsenfeld and Groudine, 2003).

3.1 DNA methylation

DNA methylation is a post-replication modification occurring mainly at the C5 position of cytosine (5mC) within CG (or CpG) dinucleotides (Figure X), though it can be also found in non-CG contexts including CHH and CHG (where H = A, C, or T) as shown in embryonic stem cells (Lister et al., 2009), oocytes, and preimplantation embryos (Imamura et al, 2005; Tomizawa et al, 2011).

Figure X. Schematic representation of DNA methylation, which converts cytosine to 5'methyl-cytosine via the action of DNA methyltransferase (DNMT).

(Adapted from Larkin et al, 2012)

Overall, mammalian genomes are depleted of CpG sites, likely as a result of mutagenic potential of 5mC that can deaminate to thymine (Bird, 1980). The remaining CpG sites are spread out across the genome where they are heavily methylated with the exception of CpG islands (Bird et al, 1985). CpG islands are stretches of DNA having a CpG density higher than the rest of the genome (Bird et al, 1985), that map to regions controlling the expression of most human genes (Saxonov et al, 2006).

DNA methylation is catalysed by DNA methyltransferase enzymes and it is known to act as a repressor of gene transcription (Kass et al, 1997). DNA methylation regulates gene silencing by preventing the binding of transcription factors to DNA (Bird and Wolffe, 1999) and by promoting the recruitment of methyl-CpG-binding domain (MBD) proteins that in turn recruit histone modifying and chromatin-remodelling complexes to methylated sites (Lopez-Serra and Esteller, 2008).

DNA methylation also plays a key role in genomic imprinting (Kacem and Feil, 2009; Smith and Meissner, 2013), as well as in the maintenance of pericentric and subtelomeric heterochromatin (Lehnertz et al, 2003; Gonzalo et al, 2006).

Differently from other modifications, DNA methylation can permanently alter the expression of genes in cells during cell division and differentiation from embryonic stem cells into specific tissues. This means that the resulting change is permanent and not reversible, in order to avoid that a differentiated cell could revert to a stem cell and then convert in another cell type. However, DNA methylation can be removed either passively, by dilution as cells divide, or by a faster, active process (Mayer et al, 2000). Active DNA demethylation can occur in both dividing and non-dividing cells but the process requires enzymatic reactions and occurs via hydroxylation of the methyl groups that are to be removed (Ito et al, 2011; He et al, 2011).

3.2 Histone modifications

Histones are the structural components of the nucleosomes, the basic unit of chromatin packaging around which the DNA wraps to form chromatin fibres. Histones are very important proteins involved especially in gene regulation. Five are the major groups of histones: H1, H2A, H2B, H3 and H4. Histones H2A, H2B, H3 and H4 are known as the core histones, while H1 is referred to as the linker histone. Two of each of the core histones are needed to create an octameric nucleosome core and approximately 150 base pairs of DNA wrap around this core particle, while the linker histone H1 binds the nucleosome at entry and exit sites of the DNA, blocking it in place (Felsenfeld and Groudine, 2003). The four core histones are relatively similar in structure and are highly conserved through evolution, having long tails on the N-terminal end which are more exposed, protruding from the centre of the nucleosome core. This tail is the location in which post-translational modifications (PTMs) appear, altering the interaction of histones with DNA and nuclear proteins (Horn and Peterson, 2002).

An extensive literature documents an elaborate collection of PTMs including acetylation, phosphorylation, methylation, ubiquitination and ADP-ribosylation that take place on the tail domains of histones (Figure XI) (Strahl and Allis, 2000).

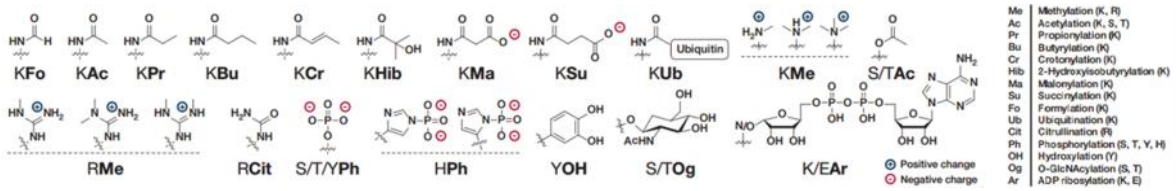

Figure XI. Snapshot of histone modifications. The histone proteins are decorated by a variety of protein post-translational modifications critical to dynamic modulation of chromatin structure and function.

(Adapted from Huang et al, 2014)

These modifications can either function to alter internucleosomal interactions, thereby affecting the higher order chromatin structure, or act as binding sites for the recruitment of chromatin-remodelling enzymes.

Histone modifications have a key role in several biological processes such as gene regulation, DNA repair, chromosome condensation (mitosis) and spermatogenesis (meiosis). For these reasons, they are often present in specific genomic regions, like promoters (regions of DNA essential for the transcriptional regulation of genes) and enhancers (regions of DNA that can be bound by proteins to activate transcription of a gene).

In particular, histone methylation is an important and widespread type of chromatin modification that is known to influence biological processes in the context of development and cellular responses. Histone methylation occurs on all basic residues: arginines, lysines and histidines. Lysines can be monomethylated (me1), dimethylated (me2) or trimethylated (me3) on their ε-amine group, arginines can be monomethylated (me1), symmetrically dimethylated (me2s) or asymmetrically dimethylated (me2a) on their guanidinyl group, and histidines have been reported to be monomethylated, although this methylation appears to be rare and has not been further characterized (Greer and Shi, 2012).

Focusing on lysine residues, the most extensively studied histone methylation sites include histone H3 lysine 4 (H3K4), H3K9, H3K27, H3K36, H3K79 and H4K20.

The trimethylation of different lysine residues of the H3 histone is associated with different extent of gene transcription. In general, the trimethylation of lysines 4, 36 and 79 (H3K4me3, H3K36me3, H3K79me3) is found predominantly in the euchromatin, while H3K27me3 and H3K9me3 modifications mark inactive genes or regions and are often termed heterochromatin modifications (Li et al, 2007).

3.3 G-quadruplex structures

G-quadruplexes are nucleic acid secondary structures, built upon the motif of the guanine quartet (Williamson, 1994). Each quartet is composed of four guanines, held together by a cyclic Hoogsten arrangement of eight hydrogen bonds. The planar G-quartets stack on top of one another forming four-stranded helical structures. G-quadruplex (G4) formation is driven by monovalent cations such as Na^+ and K^+, and hence physiological buffer conditions favour their formation (Figure XII).

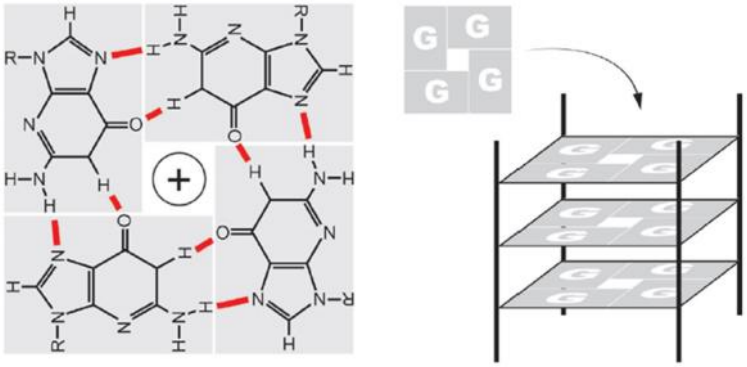

Figure XII. Structure of G-quadruplexes. The building blocks of G-quadruplexes are G-quartets that arise from the association of four guanines into a cyclic arrangement. The planar G-quartets stack on top of one another, forming four-stranded helical structures. G-quadruplex formation is driven by monovalent cations such as Na^+ and K^+.

(Adapted from Rhodes and Lipps, 2015)

G-quadruplex structures are topologically very polymorphic and can arise from the intra- or inter-molecular folding of G-rich strands. Intra-molecular folding requires the presence of four or more G-tracts in one strand, whereas inter-molecular folding can arise from two or four strands giving rise to parallel or antiparallel structures depending on the orientation of the strands in a G-quadruplex (Figure XIII) (Burge et al, 2006).

Computational analyses of the human genome searching with the consensus sequence ($G_{3+}N_{1-7}G_{3+}N_{1-7}G_{3+}N_{1-7}G_{3+}$) revealed that it contains over 300000 sequences that have the

potential to form G-quadruplexes referred to as putative G-quadruplex sequences (PQSs) (Huppert and Balasubramanian, 2005).

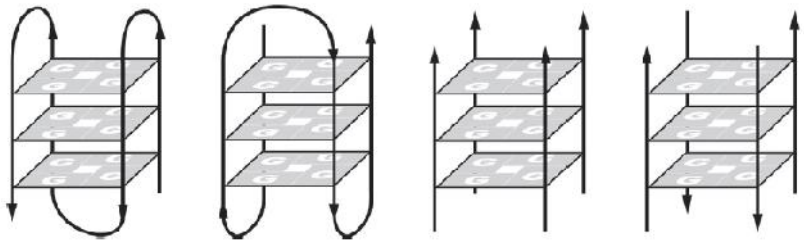

Figure XIII. Schematic diagram of the different G-quadruplex folding topologies. G-quadruplex structures are polymorphic and can be sub-grouped into different families, as for example parallel or antiparallel according to the orientation of the strands and can be inter- or intra-molecular folded.

(Adapted from Rhodes and Lipps, 2015)

The highest abundance of PQSs is at telomeres, which in humans consist of 5 to 10000 base pairs of the tandemly arranged TTAGGG repeat. They are also highly enriched in gene promoters, at the border between introns and exons and target immunoglobulin gene class switch recombination (Maizels and Gray, 2013). Most interestingly, recently it has emerged that 90% of human DNA replication origins contain PQS motifs, and in higher densities near origins that are used frequently (Figure XIV) (Besnard et al, 2012).

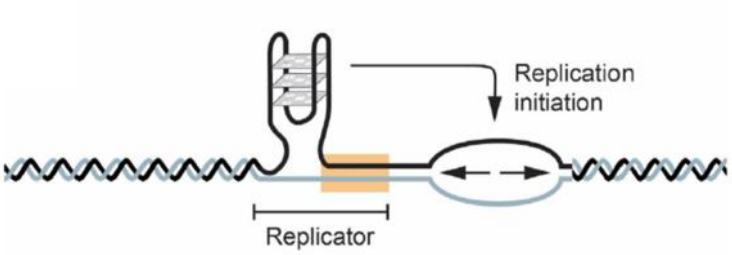

Figure XIV. G-quadruplexes and the initiation of DNA replication. Origins of replication in humans are GC-rich and contain PQS. G-quadruplex formation is required for the initiation of DNA replication and the localization of the G-quadruplex determines the site of initiation.

(Adapted from Rhodes and Lipps, 2015)

Over the last several years, the increasingly direct evidence for the presence of G-quadruplexes *in vivo,* and the identification of proteins that specifically regulate G-quadruplex folding and unfolding have started to provide insights into G-quadruplex occurrence and function. In particular, recent data suggest that G-quadruplex formation can serve both beneficial and regulatory roles in cells such as forming the capping structure of telomeres, the specification of DNA replication origins in vertebrates, and deleterious effects as they can impede the progression of replicative DNA polymerases (Rhodes and Lipps, 2015, Valton et al, 2014).

AIM OF THE THESIS

Newly designed molecules, belonging to the family of hydroxypyrones, were recently developed by coupling maltol and polyamine symmetrically.

A preliminary screening among maltol-derived compounds containing a cyclic aliphatic spacer allowed us to select maltonis (4,10-bis[(3-hydroxy-4-pyron-2-yl)methyl]-1,7-dimethyl-1,4,7,10-tetraazacyclododecane), for further investigations.

The main purposes of this study were as follows:

- to evaluate the anti-proliferative effect of maltonis and its specificity on a large panel of human tumour cell lines;
- to characterize maltonis cellular response at both biological and molecular levels;
- to investigate maltonis mechanism of action through both cellular and cell-free assays, focusing on the modulation of chromatin structure;
- to assess toxicity and therapeutic potential of maltonis by *in vivo* experiments.

MATERIALS AND METHODS

NCI-60 human tumour cell lines screen

The human tumour cell lines of the cancer screening panel were grown in RPMI 1640 medium containing 5% foetal bovine serum (FBS) and 2 mM L-glutamine. Cells were inoculated into 96 well microtitre plates in 100 µL at plating densities ranging from 5000 to 40000 cells/well depending on the doubling time of individual cell lines. After cell inoculation, the microtitre plates were incubated at 37°C, 5% CO_2, 95% air and 100% relative humidity for 24 h prior to addition of maltonis. After 24 h, two plates of each cell line were fixed in situ with trichloroacetic acid (TCA) to represent a measurement of the cell population for each cell line at the time of drug addition (Tz). Maltonis was solubilized in dimethyl sulfoxide at 400-fold the final test concentration and stored frozen prior to use. At the time of drug addition, an aliquot of frozen concentrate was thawed and diluted to twice the final test concentration with complete medium containing 50 µg/ml gentamicin. Following maltonis addition at the concentration of 10 µM, the plates were incubated for an additional 48 h at 37°C, 5% CO_2, 95% air, and 100% relative humidity. For adherent cells, the assay was terminated by the addition of cold TCA. Cells were fixed in situ by the gentle addition of 50 µl of cold 50% (w/v) TCA (final concentration, 10% TCA) and incubated for 60 min at 4°C. The supernatant was discarded, and the plates were washed five times with tap water and air dried. Sulforhodamine B (SRB) solution (100 µl) at 0.4% (w/v) in 1% acetic acid was added to each well, and plates were incubated for 10 min at room temperature (RT). After staining, unbound dye was removed by washing five times with 1% acetic acid and the plates were air dried. Bound stain was subsequently solubilized with 10 mM trizma base, and the absorbance was read on an automated plate reader at a wavelength of 515 nm. For suspension cells, the methodology was the same except that the assay was terminated by fixing settled cells at the bottom of the wells by gently adding 50 µl of 80% TCA (final concentration, 16% TCA). Using absorbance

measurements [time zero (Tz), control growth (C), and test growth in the presence of drug (Ti)], growth percentage was calculated as:

$[(Ti-Tz)/(C-Tz)] \times 100$, $Ti \geq Tz$

$[(Ti-Tz)/Tz] \times 100$, $Ti < Tz$.

Cell cultures, treatments and cell survival evaluation

Immortalized promonocytic leukaemia (U937), acute promyelocytic leukaemia (NB-4), acute myeloid leukaemia (HL-60) and T-cell leukaemia (JURKAT) human tumour cell lines were obtained from American Type Culture Collection (ATCC).

Cells were grown in RPMI 1640 (Lonza) supplemented with 10% FBS (Gibco), 1% penicillin-streptomycin (Sigma-Aldrich) and 1% glutamine (Lonza). All cell lines were grown in a humidified atmosphere at 37°C as previously described (Fanelli et al, 2008).

Bone marrow derived normal human mesenchymal stem cells (h-MSC) were obtained from patients with benign bone lesions. After washings, cells were plated in α-MEM (Lonza), supplemented with 1% penicillin-streptomycin and 20% FBS.

Maltonis was dissolved at 10 mM in double-distilled water as stock solution, stored at −80°C and subsequently diluted before use. Treatments were carried out at different concentrations (0.5, 1.0, 2.5 and 5.0 µM) and repeated every 24 h. Cellular viability was evaluated, after 72 h of treatment, by Trypan blue dye exclusion assay by using TC10 automatic cell counter (Bio-Rad). The 50% inhibitory concentration (IC_{50}) values were calculated for each cell line with CompuSyn software (ComboSyn, Inc.). The data are reported as mean ± standard deviation (SD) resulting from three independent experiments.

Cell cycle analysis and hypodiploid cells estimation

Cell cycle profiles and percentage of hypodiploid cells were studied by propidium iodide staining procedure as previously reported (Amatori et al, 2009). Cells were fixed in ice-cold 70% ethanol and stained using a propidium iodide staining solution (50 µg/ml). Cytofluorimetric acquisitions were carried out with a PAS flow cytometer (Partec) and sample analysis was carried out with FlowJo 8.6.3 software (Tree Star, Inc.). Cell cycle percent values were calculated using the Watson pragmatic model and the significance of changes was evaluated by Student's t-test.

DNA laddering assay

Following 72 h of treatment with different concentrations of maltonis (2.5 and 5.0 µM), about 2×10^6 HL-60 cells were harvested, washed once with ice-cold PBS and incubated in 2 ml of 1X TBS, 0.5% Tween-20 and 1 mM EDTA for 30 min at 4°C. Cells were centrifuged at 272*g* (1200 rpm) for 5 min at 4°C and incubated with 0.1% SDS solution for 30 min at RT in a final volume of 0.5 ml. DNA was purified using a QIAquick PCR purification kit (Qiagen), following the manufacturer's instructions, separated by 2% agarose gel electrophoresis (AGE) and detected by ethidium bromide staining.

Native chromatin extraction and DNA preparation

About 2×10^7 HL-60 cells were harvested and the final cell pellet was resuspended in 1 ml of 1X TBS. An equal volume of 1% Tween/1X TBS (v/v), containing 500 µM PhenylMethylSulfonyl Fluoride (PMSF), 2 µg/ml Leupeptin and 2 µg/ml Aprotinin, was added and the sample was incubated in rotation for 1 h at 4°C.

Cell lysate was homogenised by Dounce pestle on ice and centrifuged at 425*g* (1500 rpm) for 3 min at 4°C. Nuclei were separated on 25% sucrose/1X TBS (w/v) underlaid with a half-volume of 50% sucrose/1X TBS (w/v). After centrifugation at 714*g* (3000 rpm) for 20 min at 4°C, pelleted nuclei were resuspended in 1 ml of Digestion Buffer (0.32 M sucrose, 50 mM Tris-HCl pH 7.4, 4 mM $MgCl_2$, 1 mM $CaCl_2$, 0.1 mM PMSF, 2 µg/ml Leupeptin and 2 µg/ml Aprotinin) and the DNA concentration was measured at 260 nm.

Native chromatin was obtained by mild digestion with micrococcal nuclease (10 units of enzyme/0.5 mg chromatin) for 10 min at 37°C, and reaction was stopped by addition of EDTA (20 mM final concentration).

After pelleting by centrifugation at 13414*g* (13000 rpm) for 5 min at 4°C, the soluble chromatin was recovered from the supernatant and DNA concentration was measured at 260 nm. On average, up to 30–40% of the starting material was recovered as soluble chromatin.

DNA was obtained by digestion of extracted native chromatin with 0.5 mg/ml Proteinase K for 3 h at 45°C. At the end of digestion, DNA was purified by QIAquick PCR purification kit (Qiagen).

Histone purification

About 5×10^7 HL-60 cells were harvested, washed twice with ice-cold 1X PBS, and resuspended in Triton Extraction Buffer (TEB: PBS containing 0.5% Triton X-100 (v/v), 2 mM PMSF, 0.02% (w/v) NaN_3) at a cell density of 10^7 cells per ml. Cells were lysed on ice for 10 min with gentle stirring and successively centrifuged at 755*g* (2000 rpm) for 10 min at 4°C. Pelleted cells were resuspended in 0.2 M HCl at a cell density of 4×10^7 cells per ml and incubated over night at 4°C in slow rotation. Sample was centrifuged at 755*g* for 10 min at 4°C and histones containing supernatant was saved.

SDS/KCl Precipitation Assay

Native chromatin, DNA alone and DNA in combination with histones or bovine serum albumin (BSA) were incubated for 4 h with 4 mM maltonis or formaldehyde (as positive control) in 100 mM Tris-HCl pH 7.4. Different samples were then diluted in 2.5% SDS/1X PBS and mixed accurately. KCl was added at the final concentration of 175 mM and samples were incubated on ice for 5 min. Precipitated proteins and DNA-proteins complexes were pelleted by centrifugation at 17860*g* (15000 rpm) for 5 min at 4 °C, and supernatants, containing the unbound fractions of DNA, were collected. Pellets were washed two times in ice-cold 0.1 M KCl, 0.1 mM EDTA, 10 mM Tris-HCl pH 7.4; each wash step was followed by 5 min of incubation on ice and centrifugation at 17860*g* for 5 min at 4 °C. Supernatants obtained from each wash step were pooled with previous unbound DNA fractions. Pellets were then resuspended in 1 mL of 0.1 M KCl, 10 mM EDTA, and 40 mM Tris-HCl pH 6.5 and digested with 0.5 mg/mL proteinase K for 3 h at 45°C. After a further incubation on ice for 5 min, samples were centrifuged at 17860*g* for 5 min at 4°C and supernatants containing the bound fraction of DNA were collected. Finally, DNA contents of both bound and unbound fractions were fluorimetrically quantified by Qubit (Invitrogen).

DNA Electrophoretic Mobility Assay

Native chromatin was incubated for 4 h at 37°C with 4 mM maltonis in 100 mM Tris-HCl pH 7.4. SDS 0.1% was successively added to separate DNA from histone proteins. DNA was then analysed by 1.3% agarose gel electrophoresis and detected by ethidium bromide staining.

γH2AX immunofluorescence

After 24 hours of treatment with two different concentrations of maltonis (2.5 and 5.0 µM), HL-60 cells were cytospinned and fixed with 3.7% (v/v) formaldehyde (FA) for 5 min at RT, followed by two washes with PBS. Fixed cells were treated with 0.1% (v/v) Triton X-100 in 1X PBS/1% FBS for 10 min at RT. After 30 min of incubation at RT in FBS to prevent non-specific binding, anti-phospho-H2AX antibody (Alexa Fluor® 488 Conjugate, #9719, Cell Signaling Technology) was incubated for 1 h at RT in 1X PBS/1% FBS. Cells were then washed twice with PBS and counterstained with DAPI (diluted 1:3000) for 5 min at RT. Coverslips were then mounted on slides and images were acquired with Olympus BX50 microscope (Olympus).

Maltonis treated HL-60 cells microarray

HL-60 cells were treated with 5 µM Maltonis for 24 h or left untreated in a duplicate experiment. After treatment, cells were harvested, washed twice with ice-cold PBS and resuspended in 0.2 ml of TRIzol (Invitrogen). One hundred nanograms of total RNA were subjected to 2 cycles of cDNA synthesis with the Affymetrix WT PLUS expression kit. In the first cycle, first strand synthesis was performed using an engineered set of random primers that exclude rRNA-matching sequences and include the T7 promoter sequences. After second strand synthesis, the resulting cDNA was *in vitro* transcribed with the T7 RNA polymerase to generate a cRNA. This cRNA was subjected to a second cycle of first strand synthesis in the presence of dUTP in a fixed ratio relative to dTTP. Single strand cDNA was then purified and fragmented with a mixture of uracil DNA glycosylase and apurinic/apirimidinic endonuclease 1 (Affymetrix) in correspondence of incorporated dUTPs. DNA fragments were then terminally labelled by terminal deoxynucleotidyl transferase (Affymetrix) with biotin. The biotinylated DNA was hybridized to the Human

GeneChip® HTA 2.0 Array (Affymetrix), containing more than 285000 full length transcripts covering 44699 coding genes and 22829 non coding genes selected from *H. sapiens* genome database RefSeq, ENSEMBL and GenBank. Finally, chips were washed and scanned on the Affymetrix Complete GeneChip® Instrument System, generating digitized image data (DAT) files.

Bioinformatics analysis

Microarray analysis was performed exploiting Affymetrix Expression Console™ and Transcriptome Analysis Console software. Bioinformatics analyses were carried out through Galaxy platform (https://usegalaxy.org). Galaxy is an open, web-based platform for biological data analysis and includes interval manipulation utilities for doing set theoretic operations on intervals (*e.g.* intersection, union, etc.). Gene ontology analysis was performed using DAVID Bioinformatics Resource 6.8 (https://david.ncifcrf.gov).

Western blotting

Maltonis treated HL-60 cells were lysed in 1X Sample Buffer (62.5 mM Tris-HCl pH 6.8, 2% SDS, 0.003% bromophenol blue, 10% glycerol, 5% β-mercaptoethanol) at a cell density of 10^7 cells per ml. Fifteen microlitres of total lysates were then resolved on a 15% SDS polyacrylamide gel electrophoresis and immunoblotted with the following specific antibodies: anti-phospho-H2AX (#07-164, Millipore), anti-H2AX (#07-627, Millipore), anti-H3K9me3 (#39161, Active Motif), anti-H3 (#06-755, Upstate), anti-HP1α (#Ab9057, Abcam) and anti-αTubulin (#T9026, Sigma). Secondary goat anti-rabbit IgG, horseradish peroxidase conjugate (#G21234) and goat anti-mouse IgG, horseradish peroxidase conjugate (#G21040) were purchased from Thermo Fisher Scientific. Elaboration of

images and densitometric analysis were performed using ImageJ software (ImageJ 1.43u; National Institutes of Health).

In vivo evaluation of maltonis efficacy

To evaluate anti-tumour efficacy, non-obese diabetic (NOD)/LtSz-severe combined immunodeficiency (SCID) IL2Rγ^{null} (NSG) mice were purchased from Charles River, Italy. Eight weeks old mice were injected intravenously (iv) with 2×10^7 HL-60 cells per mouse to obtain tumour xenografts. Two days after cells inoculation mice were randomized in three groups: i) control (n = 4), ii) 5 mg/kg maltonis (n = 4) and iii) 20 mg/kg maltonis (n = 4). Treated group mice received maltonis daily intra-peritoneally (ip) for 5 days per week, while control group mice were treated with vehicle alone (PBS).

Animal experiments were performed according to European directive 2010/63/UE and Italian law 26/2014. Experimental protocols were reviewed and approved by the Institutional Animal Care and Use Committee of the European Institute of Oncology, and forwarded to the Italian Ministry of Health.

Ki-67 evaluation

Detection of Ki-67 was performed on sections pre-treated with a citrate buffer solution (0.01 M citric acid and 0.01 M sodium citrate pH 6.0) in a microwave oven at 750 W and stained with the anti-human Ki67 antibody (Clone MIB-1, #M7240, Dako).

RESULTS

1. Evaluation of maltonis anti-proliferative effects

A preliminary cancer drug screening, conducted on several maltol-derived compounds containing a cyclic aliphatic spacer, allowed us to select maltonis (4,10-bis[(3-hydroxy-4-pyron-2-yl)methyl]-1,7-dimethyl-1,4,7,10-tetraazacyclododecane) for further biological investigations.

1.1 NCI-60 human tumour cell line anti-cancer drug screen

Maltonis was submitted to National Cancer Institute (NCI) USA, for the NCI-60 human tumour cell lines screening in order to assess anti-proliferative effect and potential specificity of the compound. The screen was implemented in fully operational form in 1990 in order to identify and characterize novel compounds able to inhibit or kill tumour cells. The screen consists of 60 different human tumour cell lines, representing leukaemia, melanoma, lung, colon, brain, ovarian, breast, prostate, and kidney cancers (Monks, 1991).

In the one dose (10 μM) NCI-60 screening, maltonis showed potent anticancer activity towards several cancer cell lines of different origin with a global growth inhibition (GI) value of 46.29% (Figure 1).

Moreover, a deeper characterization of NCI-60 results allowed us to find a significant inverse correlation between maltonis growth inhibitory effect and cell lines doubling time with a Pearson's correlation coefficient of -0.53 and a p-value less than 10^{-4} (Figure 2).

In light of the data obtained by single dose NCI-60 screening, we focused our research on haematological malignancies as leukaemia cell lines proved to be among the most sensitive to maltonis treatments with an average GI value of 58.88% (± 9.91%).

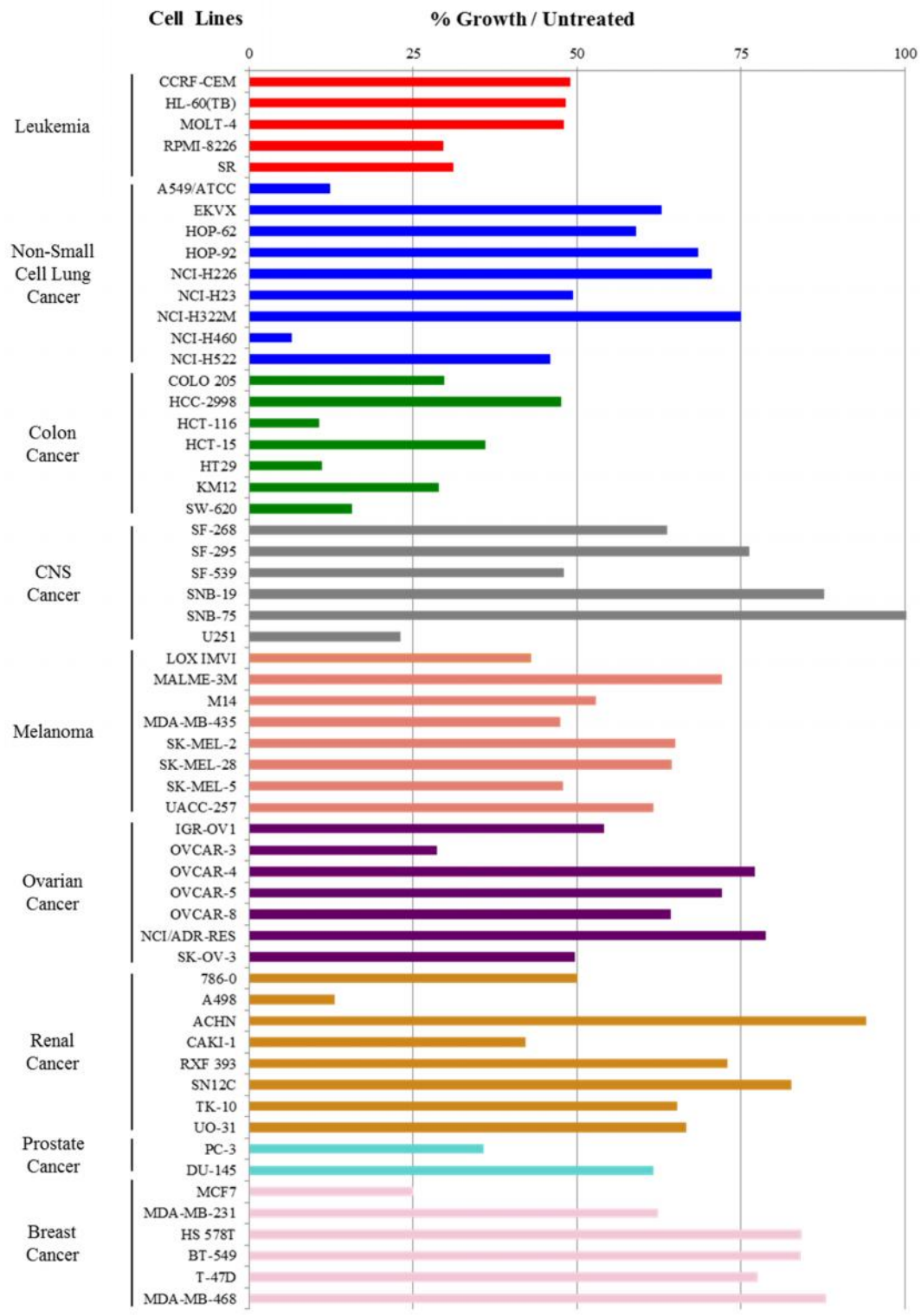

Figure 1. Maltonis inhibited growth of various cancer cell lines. Maltonis was screened exploiting the Developmental Therapeutics Program (DTP) from the National Cancer Institute (NCI/NIH). Maltonis was incubated for 48 hours with 58 different cancer cell lines at a concentration of 10 μM, and percentage cell growth was measured and compared to untreated samples. Analyses were done as described at http://dtp.cancer.gov/discovery_development/nci-60.

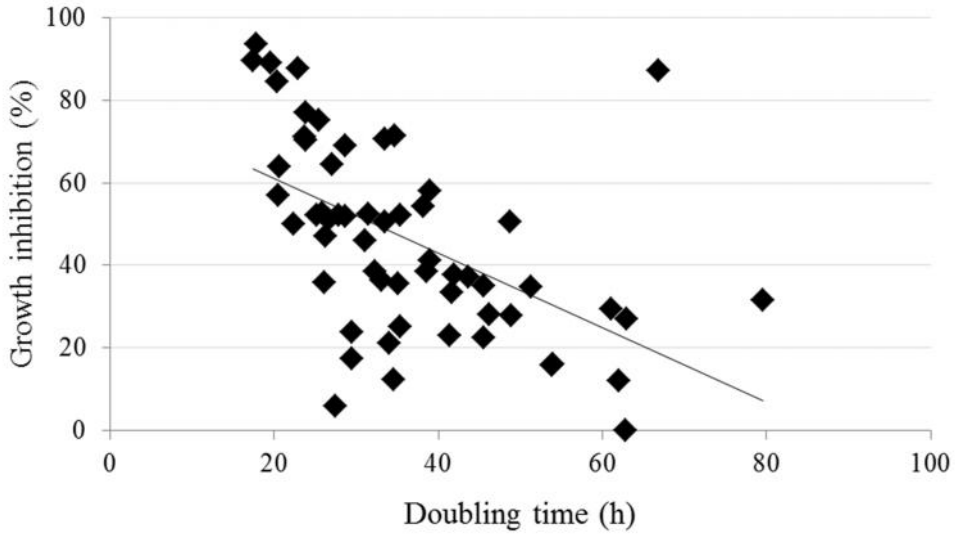

Figure 2. Maltonis growth inhibition is dependent on cell lines doubling time. The graph shows the inverse correlation between maltonis inhibitory effect and cancer cell lines doubling time. Each symbol represents a cell line in the NCI-60 panel. Pearson's correlation coefficient = −0.53, p-value < 10^{-4}.

1.2 Characterization of maltonis response in haematopoietic cell lines

In order to further characterize the response of hematopoietic cells to maltonis treatment, U937, NB-4, JURKAT and HL-60 cell lines were subjected to 72 hours of exposure in dose-response experiments.

We found that treatments with maltonis at concentrations ranging from 0.5 to 5.0 µM result in a dose-dependent reduction in cell survival (Figure 3). The IC_{50} value was calculated for each cell line showing no appreciable variations among the lines tested with an average IC_{50} value of 1.53 ± 0.37 µM.

In addition, as already reported (Guerzoni et al, 2014), two human bone marrow derived mesenchymal stem cells were used to assess the effects of maltonis on normal cell growth. Interestingly, human mesenchymal stem cells appeared to be unaffected by the compound with an IC_{50} value higher than 50 µM.

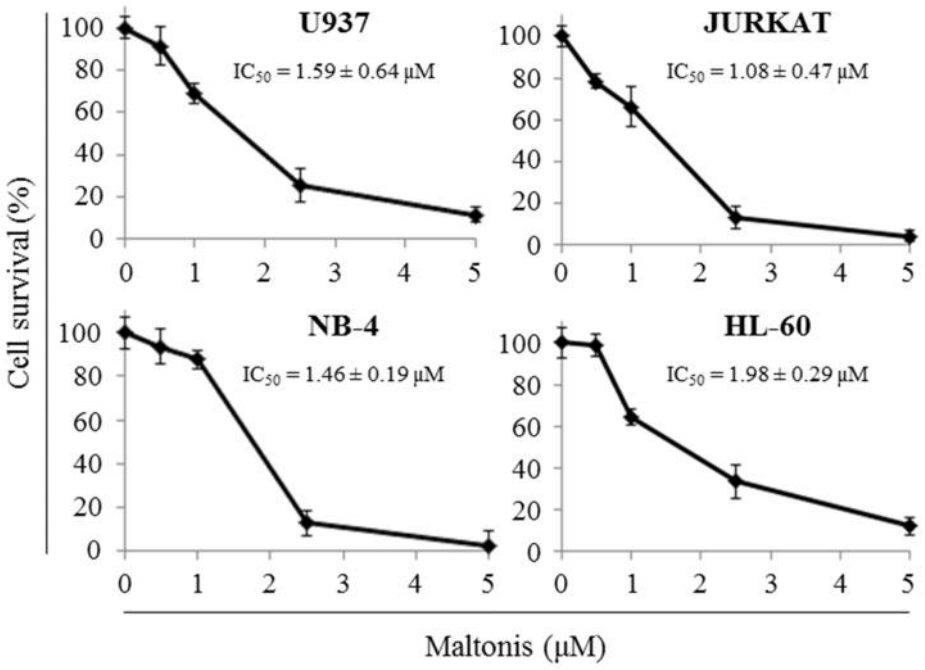

Figure 3. Dose-response experiments on U937, JURKAT, NB-4 and HL-60 tumour cell lines. Reduction of cell survival induced by maltonis treatments in four haematopoietic tumour cell lines. Cells were treated for 72 hours with the reported concentrations of maltonis and analysed by Trypan blue dye exclusion assay. The data are reported as mean ± standard deviation (SD) resulting from three independent experiments.

The biological response to maltonis was further detailed by analysing the effects on cell cycle progression. Maltonis treatments of 72 hours at concentrations of 0.5, 1.0 and 2.5 µM induced cell cycle perturbations that were monitored in all the cell lines considered in this study. The effect was dose-dependent and was characterised by the accumulation of cells mainly in G2-M phase (Figure 4 and Table 1).

In order to investigate the effects mediated by maltonis, programmed cell death was evaluated after 72 hours of treatment monitoring the hypodiploid cells percentage. A clear increase in such percentage was observed at 5.0 µM of maltonis concentration and no significant differences were noticed between the cell lines tested (Figure 5A).

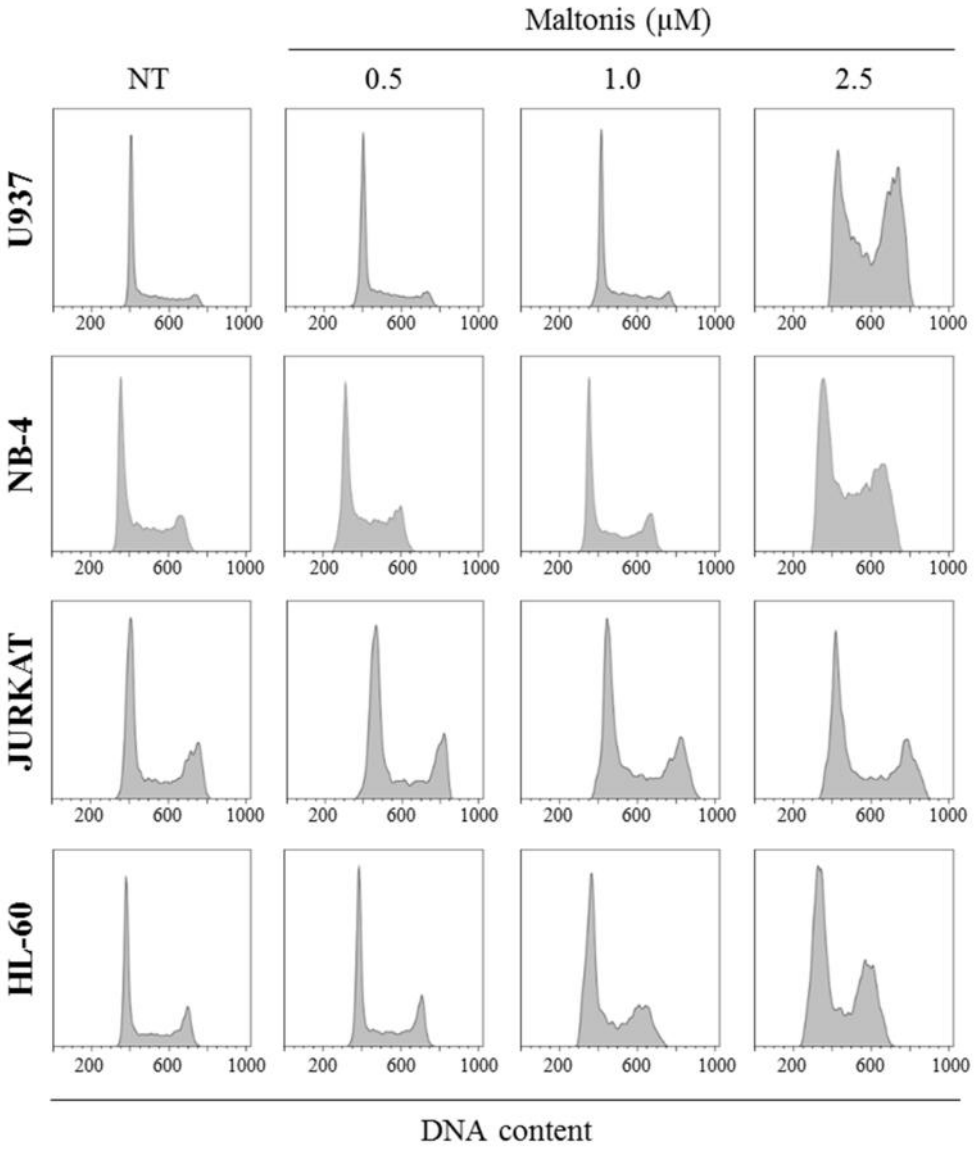

Figure 4. Cell cycle alterations induced by maltonis treatments. Cells were exposed for 72 hours to the reported concentrations of maltonis or left untreated. Cell cycle profiles have been evaluated by flow cytometric analysis of propidium iodide-stained cells. NT, Not treated.

The activation of the apoptotic programme was subsequently confirmed by analysing the internucleosomal DNA fragmentation induced by maltonis exposure in HL-60 cells, at concentrations of 2.5 and 5.0 μM (Figure 5B).

Cell Lines	µM	% G1	% S	% G2-M
U937	—	46.4 ± 3.7	48.1 ± 5.2	4.4 ± 1.5
	0.5	47.6 ± 4.1	44.9 ± 3.8	5.4 ± 1.8
	1.0	42.0 ± 4.9	47.4 ± 3.9	3.7 ± 1.8
	2.5	30.0 ± 4.2*	44.1 ± 4.1	27.2 ± 2.7*
NB-4	—	29.3 ± 2.5	57.7 ± 4.1	12.2 ± 1.9
	0.5	32.7 ± 3.0	55.9 ± 3.8	8.6 ± 3.1
	1.0	34.2 ± 3.8	52.2 ± 3.3	12.3 ± 2.2
	2.5	29.1 ± 4.7	50.6 ± 5.3	22.4 ± 3.4*
JURKAT	—	44.5 ± 3.5	38.2 ± 3.8	18.8 ± 1.7
	0.5	39.8 ± 4.4	38.5 ± 4.3	21.5 ± 2.4
	1.0	36.0 ± 2.6*	39.9 ± 5.2	22.2 ± 2.1
	2.5	35.7 ± 2.9*	38.7± 4.2	24.8 ± 1.9*
HL-60	—	41.7 ± 3.6	43.0 ± 2.8	12.4 ± 1.2
	0.5	40.3 ± 4.2	44.8 ± 3.7	13.6 ± 2.4
	1.0	40.7 ± 2.9	39.7 ± 3.6	18.8 ± 2.3*
	2.5	42.6 ± 2.7	34.5 ± 2.0*	23.2 ± 3.1*

Table 1. Cell cycle modifications induced by maltonis treatments. Data represent mean values ± standard deviation of three independent experiments. *Statistically relevant variations respect to untreated controls (Student's t test, $P < 0.05$).

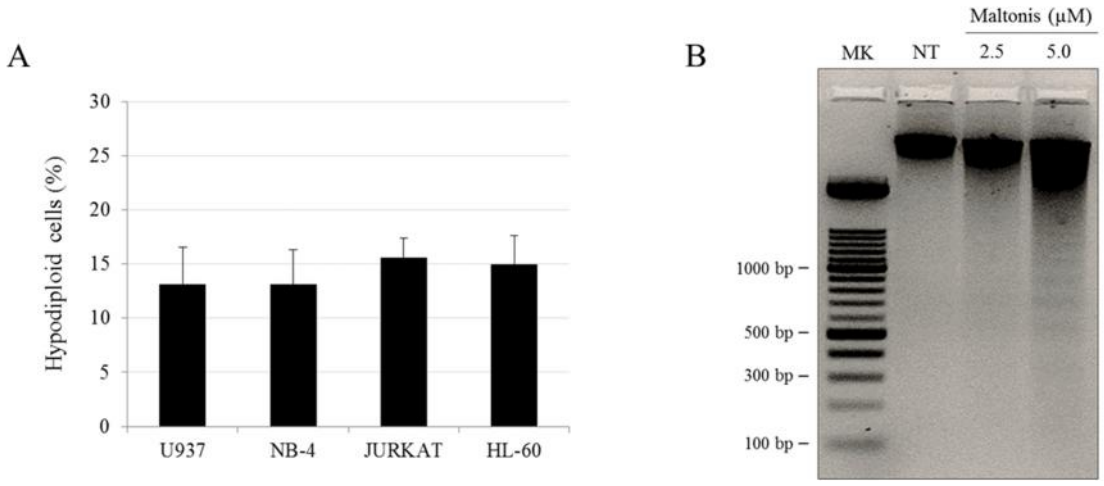

Figure 5. Maltonis-mediated induction of programmed cell death. (A) Percentage of hypodiploid cells induced by 72 hours of maltonis treatment at the final concentration of 5.0 µM. Hypodiploidy was evaluated by flow cytometric analysis of propidium iodide stained cells. The data are reported as mean ± SD resulting from three independent experiments. (B) Apoptosis-related DNA fragmentation induced by 72 hours maltonis exposure in HL-60 cells at the final concentration of 2.5 and 5.0 µM. NT, Not treated; MK, Marker.

In light of the *in vitro* results, that showed comparable IC_{50} values among the four lines tested, and considering datasets available in literature, we decided to choose HL-60 cells as representative experimental model for the following experiments.

2. Study of maltonis mechanism of action

Previous studies on malten, another maltol-derived compound, revealed its ability to induce complex structural alterations of genomic DNA due to the generation of DNA inter-molecular cross-linking (Amatori et al, 2010).

Thus, we investigated the potentiality of maltonis to interfere with chromatin structure so as to understand whether the formation of covalent bonds could mediate the effect monitored on the different cell lines.

2.1 Analysis of chromatin structural modifications induced by maltonis

To analyse the hypothesised action of maltonis, we exploited two different cell-free assays: SDS/KCl precipitation and agarose gel electrophoresis.

Native chromatin, DNA alone and DNA in combination with histones or bovine serum albumin (BSA) were incubated for 4 hours with 4 mM maltonis and then fractionated by SDS/KCl precipitation as described in the Materials and methods section. Formaldehyde (FA) treatment was used as positive control of crosslinking as FA is known to induce cross-linking of primary amino groups in proteins with other nearby nitrogen atoms in protein or DNA through a $-CH_2-$ linkage (Solomon and Varshavsky, 1985).

A significant increase of DNA in protein-bound fractions was observed both in native chromatin and DNA plus histone samples treated with maltonis while no increases were observed when maltonis was added in DNA alone or DNA plus BSA samples (Figure 6A). These results suggest that in order to perform covalent bonds, maltonis could require DNA and proteins spatial proximity, as exemplified by native chromatin structure and to a less extent achievable, through electrostatic interactions, in DNA plus histones samples.

The DNA-protein binding activity of maltonis was then further investigated on native chromatin through a canonical agarose gel electrophoretic assay. We showed that, despite SDS incubation, maltonis treatment was able to impair electrophoretic migration of DNA whereas no alteration was visible in untreated sample run (Figure 6B).

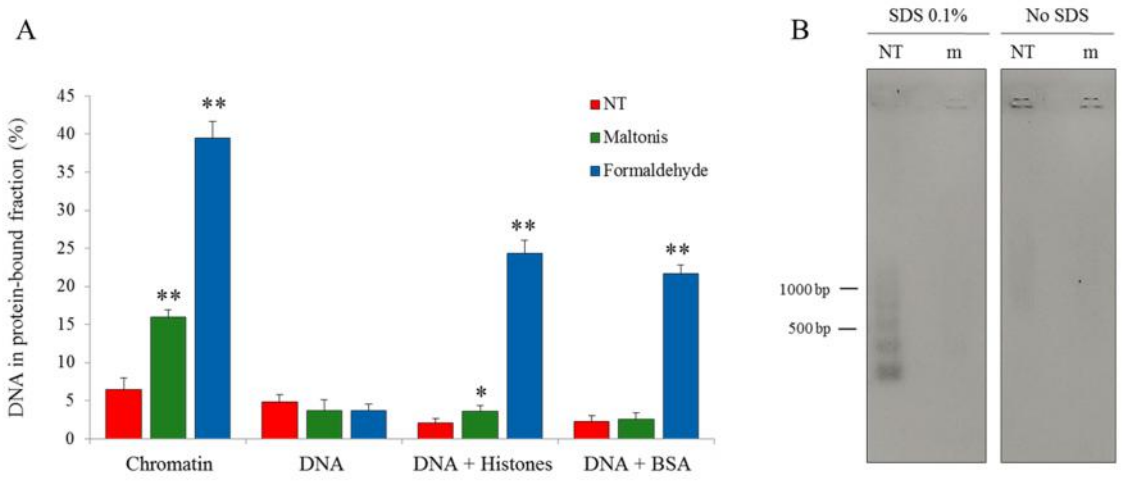

Figure 6. DNA-protein binding activity of maltonis. (A) SDS/KCl precipitation assay. Native chromatin, DNA alone and DNA in combination with histones or BSA were treated for 4 hours with 4 mM maltonis or formaldehyde (as positive control) and then fractioned by SDS/KCl precipitation. The amount of DNA in protein-bound fractions was fluorimetrically quantified. *P < 0.05, **P < 0.01 respect to untreated samples by Student's t test. (B) Impaired electrophoretic mobility of chromatin. Native chromatin was treated for 4 hours with 4 mM maltonis, incubated or not in 0.1% SDS solution and separated by agarose gel electrophoresis. SDS, Sodium dodecyl sulfate; NT, Not treated; m, Maltonis.

Taken together, these observations demonstrate that maltonis is able to induce covalent protein-DNA binding, thus altering chromatin structure.

2.2 Evaluation of DNA damages induced by maltonis

In light of the cell-free assay results, we hypothesised that covalent cross-links induced by maltonis treatments could underlie the formation of DNA double-strand breaks and activate DNA-damage response (DDR).

Therefore, we assessed, by an immunofluorescence approach, the phosphorylation of histone H2AX (γH2AX) as marker of DDR on HL-60 cells. We detected an increase of γH2AX marker at 24 hours of treatment with two different concentrations of maltonis (2.5 and 5.0 µM) (Figure 7A).

We confirmed this result by performing a western blot analysis of phosphorylated H2AX histone. A dose-dependent increase was monitored in HL-60 cells treated for 24 hours with maltonis (+6.74 fold at 2.5 µM and +8.19 fold at 5.0 µM of maltonis respect to untreated control, Figure 7B).

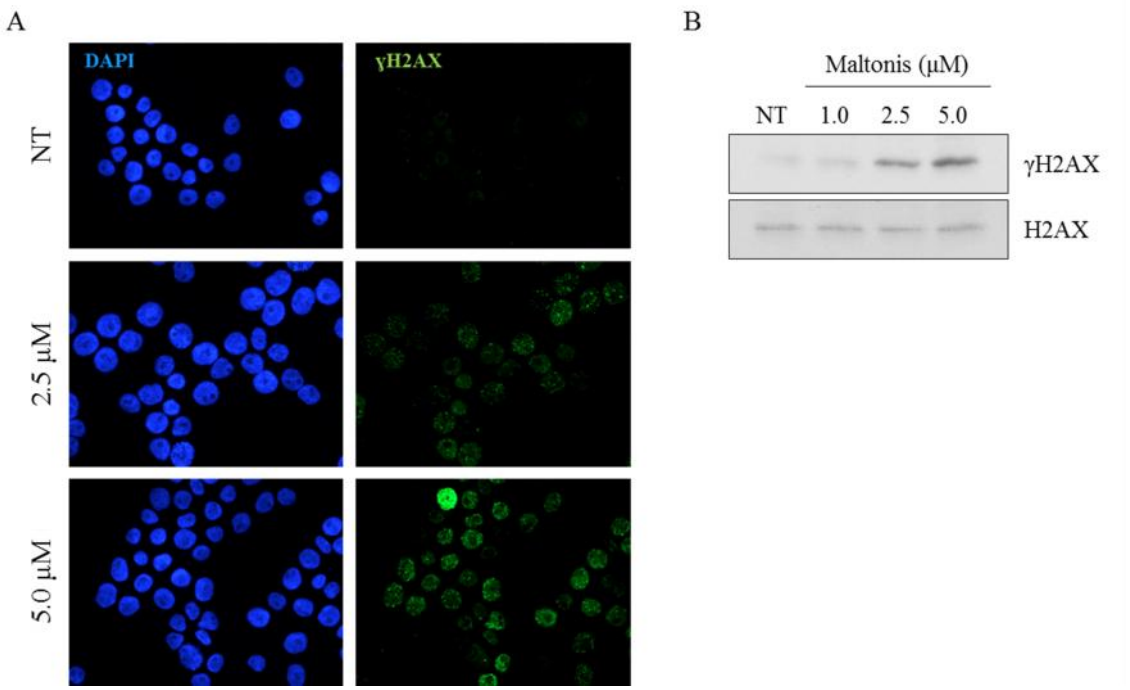

Figure 7. Maltonis treatment induces DNA damage response activation. (A) Induction of H2AX phosphorylation (γH2AX) in HL-60 cells after exposure for 24 hours to 2.5 and 5.0 µM maltonis (magnification × 40). (B) Western blot analysis of cell lysates obtained from maltonis-treated and untreated HL-60 cells. DAPI, 4',6-Diamidino-2-phenylindole dihydrochloride; NT, Not treated.

2.3 Gene expression profile of maltonis-treated HL-60 cells

To better define the molecular response triggered by maltonis, we evaluated gene expression profile of maltonis-treated HL-60 cells by a microarray analysis using an

untreated sample as reference.

We carried out the experiment in duplicate exposing HL-60 cells to 5.0 µM maltonis for a short-time (24 hours), so as to avoid apoptotic programme activation.

DNA microarray is a high-throughput technique that permits the analysis of several thousands of genes in one single experiment, providing a snapshot of the gene expression profile resulting from a drug treatment (Cheung et al, 1999; Duggan et al, 1999).

In our experiments, we used the GeneChip® Human Transcriptome Array 2.0, which allows the differential expression analysis of 67528 transcript clusters, 44699 coding and 22829 non-coding regions. To normalize, perform data quality control, and summarize data from tens of thousands of genes, we exploited the Affymetrix Expression Console™ software.

The Principle Component Analysis (PCA) as well as the Pearson's correlation plot showed a clear distinction between the maltonis-treated and the untreated samples (Figure 8), thus giving a first hint regarding the capability to distinguish different features in maltonis-treated HL-60 cells.

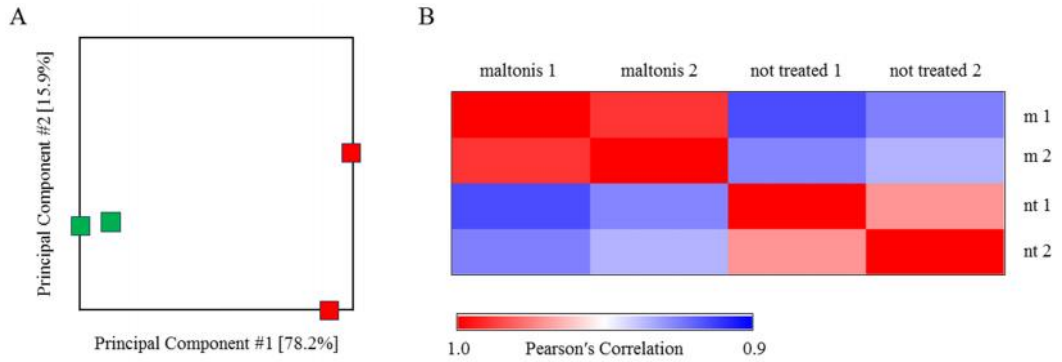

Figure 8. Principal component analysis and Pearson's correlation graph. (A) PCA plot was performed using normalized data obtained by DNA microarray analysis of maltonis-treated (green squares) and untreated (red squares) HL-60 cells. Principal components 1 (PC1) and PC2 values are reported in graph. (B) Pearson's correlation matrix of normalized DNA microarray data.

To perform further analysis of the data, we used the Transcriptome Analysis Console (TAC) software by Affymetrix so as to obtain a list of differentially expressed genes. We used the unpaired one-way between-subject ANOVA algorithm applying two filter criteria: a fold change threshold equal to 2 and an ANOVA p-value lower than 0.05.

Setting these parameters, we selected 3491 genes differentially expressed in maltonis treated HL-60 cells respect to the untreated controls. Out of 3491 genes, 2503 were up-regulated by maltonis treatment while 988 were down-regulated (Figure 9).

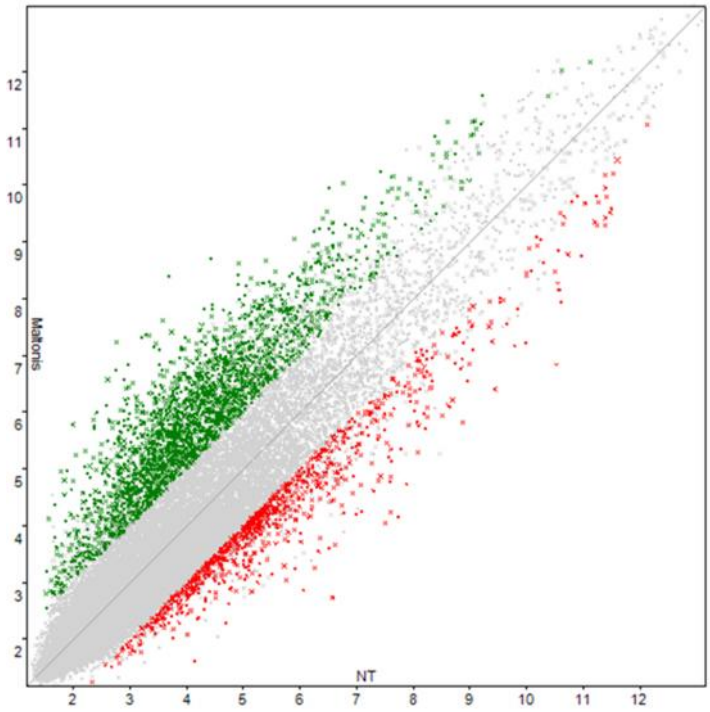

Figure 9. Scatter plot. Scatter plot depicts the expression levels (calculated as $\log_2$) in maltonis-treated and untreated HL-60 cells. Genes whose expression levels are identical in the two conditions are located on the bisector. Green crosses represent transcripts up-regulated following maltonis treatment, whereas red crosses symbolize the ones down-regulated. Genes showing a regulation exceeding the 2-fold criterion and an ANOVA p-value < 0.05 were considered as differentially expressed. NT, Not treated.

We then used the Database for Annotation, Visualization and Integrated Discovery (DAVID) analytic tools to identify enriched biological themes by Gene Ontology (GO) analysis (Huang et al, 2009).

Differentially expressed genes selected by filter criteria were analysed and the main gene ontology categories involved in maltonis response are showed in figure 10.

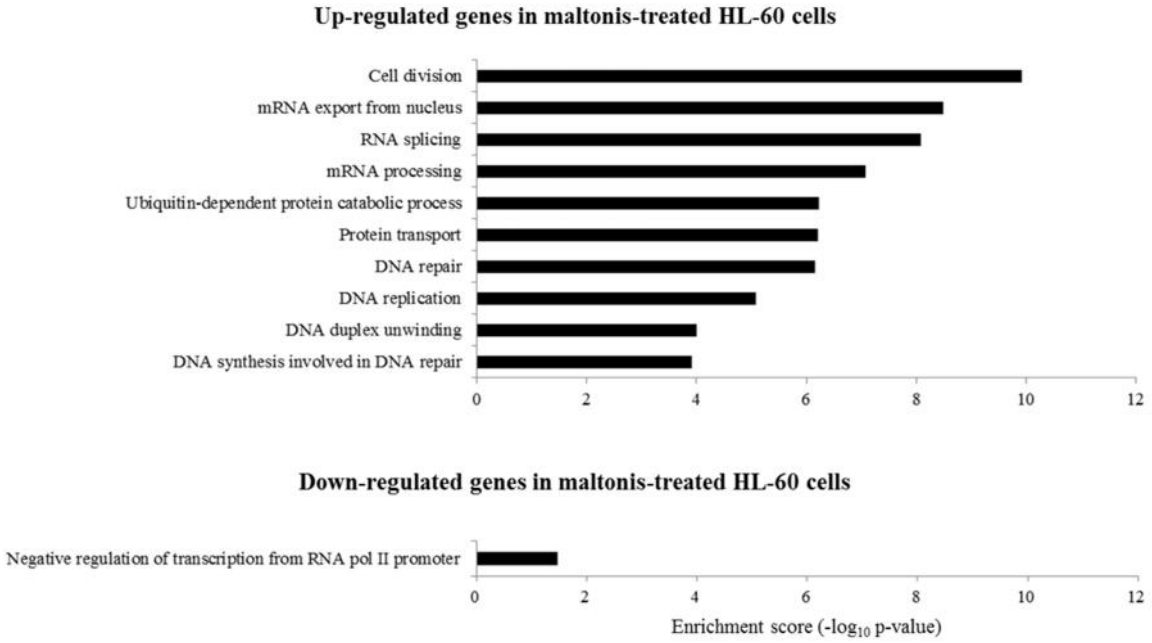

Figure 10. Gene ontology (GO) analysis of regulated genes in maltonis-treated HL-60 cells. GO analysis was performed using the 'Functional Annotation Tool' in DAVID (http://david.ncifcrf.gov/) and biological process terms are indicated. Pathways with a p-value greater than 0.05 were filtered out. The top 10 pathways are shown for the up-regulated genes, while, for the down-regulated genes, the only process that matched the p-value criterion is plotted.

In agreement with previous data, the expression of genes involved in cell division and DNA repair was affected in response to maltonis treatment. The analysis revealed the up-regulation of several cyclin and cyclin-dependent kinase genes (*e.g.* CCNT1, CCNL1, CCNH, CDK6, CDK12, etc.). Likewise, ATM (Ataxia telangiectasia mutated**)**, ATR (Ataxia telangiectasia and Rad3 related) and many other genes implicated in DDR activation was considerably up-regulated.

Strikingly, mRNA processing, splicing and export from nucleus were among the most enriched pathways, suggesting a strong maltonis-mediated effect on RNA regulation.

In addition, genes involved in DNA unwinding process were up-regulated in maltonis treated HL-60 cells, thus supporting the hypothesis that maltonis induced crosslinking could play a role in the anti-proliferative effect observed in *in vitro* experiments.

Conversely, the negative regulation of transcription from RNA polymerase II promoter was the only gene ontology category enriched among the down-regulated genes.

Furthermore, a deep analysis of the chromosome summary graph, obtained by TAC software, allowed us to identify the accumulation of down-regulated (DR) genes in specific chromosomes in a percentage higher than the random expected distribution dependent by the size of chromosomes (Figure 11).

Figure 11. Chromosome summary of down-regulated genes in maltonis-treated HL-60 cells. Map of down-regulated transcript positions along chromosomes (black square). The size of each chromosome summary square represents its gene size. In some instances, a square appears larger because it may contain multiple probe sets due to minimal pixel limitation. Chromosomes 16, 17, 19 and 22 are distinctly enriched in down-regulated transcripts.

2.4 Analysis of down-regulated genes distribution

Remarkably, as stated above, the distribution of DR genes upon maltonis treatments was partially related to specific regions of chromosomes and the majority of DR genes were not functionally regulated.

A bioinformatics analysis showed a strong correlation between DR genes and GC-rich regions. As shown in Figure 12, GC percentage was higher in body of DR genes compared to reference standard (RefSeq) genes (55.34% and 41.97%, respectively). In addition, we calculated the GC percentage also in up-regulated (UR) genes, showing in this case a comparable value respect to RefSeq genes. The same analysis was repeated evaluating GC% profile around the transcription start site (TSS ± 2.5 kb) of genes. Again, we monitored the same trend previously observed for gene bodies (Figure 12).

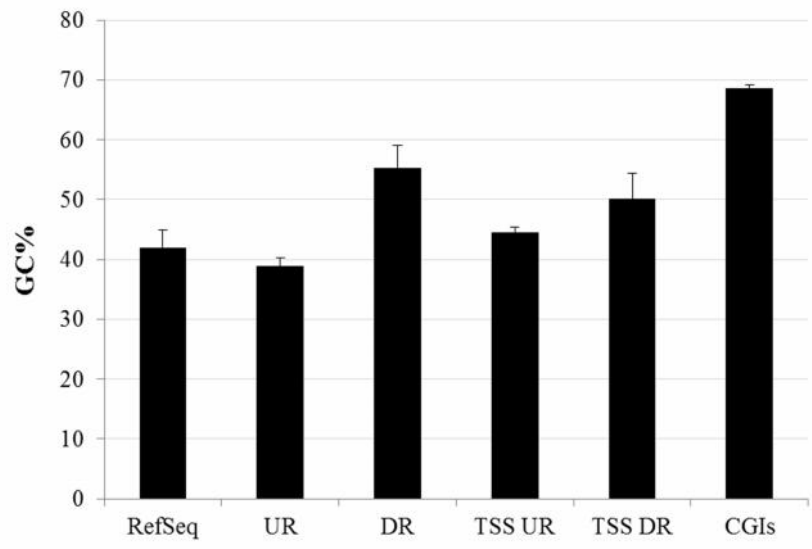

Figure 12. Maltonis treatment induces down-regulation of GC-rich genes. The histogram depicts GC percentage over the indicated regions. Both gene bodies and transcription start sites of down-regulated genes (indicated as DR and TSS DR, respectively) are enriched in GC content respect either to RefSeq or up-regulated genes (UR). CpG islands (CGIs) were considered as GC-rich regions. RefSeq defines genomic sequences to be used as reference standards for well-characterized genes.

The attractive hypothesis that maltonis could function interacting with specific features of chromatin structure was further investigated by analysing the correlation of DR genes with genome sequences prone to adopt G-quadruplex DNA structures. By comparing our data with that obtained by Rodriguez *et al* (2012), we calculated the percentage of DR genes that contained a putative-quadruplex sequences (PQSs) percentage higher than the whole-transcriptome median value 0.257%. PQS% represents the percentage of bases of a gene that are located within the PQSs mapped by the Quadparser algorithm (Huppert and Balasubramanian, 2005). As shown in figure 13, about 87% of DR genes contain a PQS% higher than the median value, while only 15% of UR genes fall into the same group.

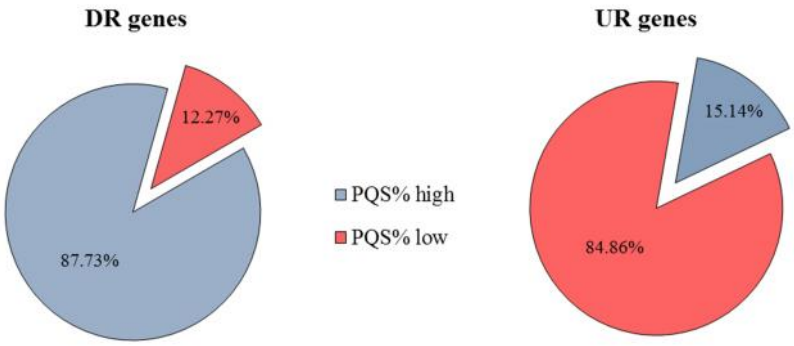

Figure 13. Down-regulated genes mainly lie within putative G-quadruplex regions. Pie charts show the percentages of down- and up-regulated genes (DR and UR, respectively) that lie within putative G-quadruplex sequences (PQSs). The majority of DR genes fall into genomic regions that have a PQS percentage higher than the median value (PQS% high) whereas just a small percentage of UR genes fall into the same group.

Overall, these results suggest a potential affinity of maltonis towards GC-rich regions with a particular propensity to recognize G-quadruplex structures.

Recent evidence showed that G-quadruplex sequence motifs are prevalent in the human genome and are enriched in gene regulatory regions and gene bodies, and in repetitive sequences, such as telomeres (Todd et al, 2005; Verma et al, 2008).

Thus, we tried to evaluate whether the affinity of maltonis towards G-quadruplex structures could influence specific features of telomeres.

In particular, we focused on the trimethylation at lysine 9 of histone H3 (H3K9me3) and on the related Heterochromatin protein 1 alpha (HP1α, also called CBX5).

H3K9me3 mark and HP1 proteins are commonly found in constitutive heterochromatin and are enriched at telomeres where they may contribute to further compaction of telomeric and subtelomeric regions (Majocchi et al, 2014).

We carried out a western blot analysis on HL-60 cell lysates, following a 24 hours treatment with 2.5 and 5.0 µM of maltonis (Figure 14). Interestingly, we noticed a decrease, at 5.0 µM of maltonis treatment, in the signal of both H3K9me3 mark and HP1α protein (−3.41 fold and −1.91 fold respect to untreated control, respectively).

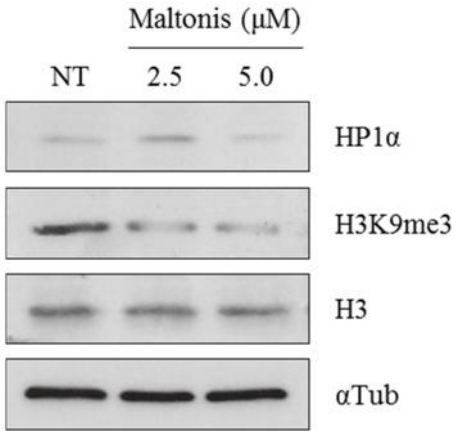

Figure 14. Maltonis treatment reduces HP1α protein levels and inhibits H3K9 trimethylation. Western blot analysis of cell lysates obtained from maltonis-treated and untreated HL-60 cells. NT, Not treated.

These results support the hypothesis of a potential interference on telomeric structures related to covalent bonds induced by maltonis.

3. *In vivo* evaluation of maltonis efficacy

In a first pilot experiment, we evaluated the therapeutic potential and toxicity of maltonis in a human AML (HL-60) xenograft murine model.

Non-obese diabetic (NOD)/LtSz-severe combined immunodeficiency (SCID) IL2Rγ^{null} (NSG) mice were intravenous inoculated with 2×10^7 HL-60 cells to mimic the invasiveness and proliferative capacity of primary AML, leading to the disseminated growth of tumour cells and ultimately to death within 4-5 weeks (Agliano et al, 2008). Two days after cell injection, mice were divided into three subgroups (n=4, for each group): control mice were treated with vehicle alone (phosphate buffered saline, PBS), whereas treated mice received injection of maltonis, at two different concentrations (5 mg/kg and 20 mg/kg), once a day for 5 days per week. Intraperitoneal (ip) drug administration was chosen as first attempt in order to administer large volumes of fluid simply and safely. At the indicated doses, maltonis was very well tolerated: we did not observe any significant changes in mice weight, blood glucose and urea levels or other signs of collateral toxicity. Preliminary results showed a slight but significant (p-value less than 0.05) increase in the overall survival time of mice treated with 20 mg/kg of maltonis while no significant differences were observed in the group treated with 5 mg/kg of maltonis. In particular, the mean survival time for control mice was 34.7 (± 0.5) days, while the mean survival times in treated groups were estimated to be 35.7 (± 1.2) days and 37.5 (± 0.6) days for 5 mg/kg and 20 mg/kg of maltonis, respectively.

Moreover, as HL-60 cells generated abdominal solid tumours, we evaluated the proliferation marker Ki67 expression in histological tissues of control and treated mice, showing Ki67 inhibition at high concentrations of maltonis (Figure 15).

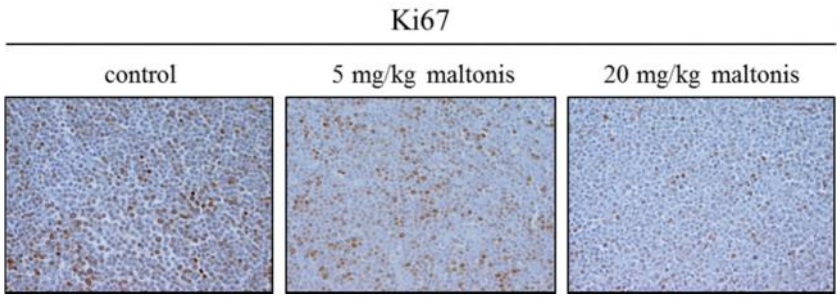

Figure 15. Maltonis anti-proliferative effect in human AML (HL-60) xenograft murine model. Representative immunohistochemical evaluation of Ki67 in control and maltonis-treated tumour (magnification × 200).

DISCUSSION

Despite increasing advances in modern treatments for tumours, the survival of many patients affected by cancer remains extremely poor. The high possibility of relapse, the absence of specific therapies and resistance to standard chemotherapy represent the main causes of failure in cancer treatment (Tobias and Hochhauser, 2010). Thus, there is an urgent necessity for research focused on the identification and description of new anti-tumour agents.

In this study, we provide the biological properties of a new synthetic maltol-derived molecule, maltonis, and the preliminary attempts to understand its molecular mechanism of action.

The sensitivity to maltonis exposure of several tumour cell lines of different origin was assayed through NCI-60 human tumour cell lines screen, highlighting a correlation between maltonis biological effect and cell lines doubling time. Subsequently, focusing on haematopoietic cell lines (U937, HL-60, NB-4 and JURKAT), we showed that maltonis is able to drastically reduce the cell survival of the four cell lines tested, and to induce programmed cell death and cell cycle perturbations. High doses of maltonis activated the apoptotic cellular response, whereas sublethal treatments induced the accumulation of cells mainly in G2-M phase.

The late S and G2-M block is usually associated with compounds known to form adducts with DNA and currently included in several therapeutic protocols (Siddik, 2003). As a consequence of these observations, the possible DNA structural alterations induced by maltonis have been investigated by cell-free studies. We showed that maltonis exposure induces the formation of covalent bonds at the chromatin level strongly impairing DNA electrophoretic mobility.

Interestingly, a similar interference has been already described for some DNA alkylating

compounds (Pereira et al, 1998; David-Cordonnier et al, 2002; Novakova et al, 2009) and it has been associated with the formation of a DNA matrix of high molecular weight, which results from the inter-helical crosslinking of multiple DNA molecules.

In light of these results, we investigated whether maltonis physical interaction with the chromatin structure was sufficient to alter nucleic acid properties and recruit the DNA repair system. Formation of γH2AX nuclear foci was observed in HL-60 cells following a short treatment with maltonis, revealing the recruitment of DNA damage response (DDR) machinery likely due to cross-linking induced DNA double strand breaks (DSBs). DDR activation was also confirmed by microarray-based comparative gene expression analysis of maltonis treated HL-60 cells, that showed an up-regulation of DNA repair genes.

Moreover, in accordance with the observed cell cycle perturbations, gene ontology (GO) analysis revealed cell division as a major pathway regulated by maltonis treatment. Likewise, genes involved in RNA processing, DNA synthesis and DNA replication were in the top ten GO categories of maltonis regulated genes, further supporting the hypothesis of a possible interference closely related to the maltonis ability to interact with nucleic acids.

Maltonis-mediated regulation of DNA replication genes is in agreement with the correlation found in the previous analysis of NCI-60 screening between maltonis growth inhibitory effect and cell lines doubling time.

Conversely, GO analysis of genes down-regulated by maltonis treatment highlighted the negative regulation of transcription from RNA polymerase II promoter as the only significant GO category. Furthermore, down-regulated genes genome-wide distribution was proved to be dependent on GC-rich regions and G-quadruplex structures.

Taken together, these results suggest that the negative regulation of genes observed in microarray analysis could be related, at least partially, to maltonis-mediated crosslinking at the chromatin level.

In addition, recent evidence demonstrated that GC content and genomic distribution of G-quadruplex motifs are highly correlated with telomeric regions and replication origin locations (Besnard et al, 2012; Cayrou et al, 2012; Rhodes and Lipps, 2015). In particular, Besnard and co-authors propose a model in which the specific distribution of G4 motifs in the human genome is involved in both origin selection and efficiency, constituting a driving force for establishment of the spatiotemporal programme of replication.

Therefore, the possibility that maltonis interaction with GC-rich sequences and G-quadruplex structures might affect DNA replication and/or telomere maintenance could represent an intriguing mechanistic hypothesis, worthy to be further investigated.

The *in vitro* efficacy of maltonis was also tested *in vivo* on a human AML (HL-60) xenograft murine model. In a preliminary experiment, treatments with maltonis at the concentration of 20 mg/kg produced a significant increase in the survival time of xenograft mice. Cell proliferation inhibition was observed, thus substantially confirming results obtained *in vitro*.

Current experiments aim to better define the sites of maltonis interaction, by γH2AX chromatin immunoprecipitation followed by high throughput sequencing (ChIP-seq), and to further evaluate *in vivo* maltonis anti-cancer potential.

Overall, although additional investigations will be necessary, results obtained in this study suggest a potential role for maltonis as anti-cancer agent.

REFERENCES

Agliano, A., Martin-Padura, I., Mancuso, P., Marighetti, P., Rabascio, C., Pruneri, G., Shultz, L. D., and Bertolini, F. (2008). Human acute leukemia cells injected in NOD/LtSz-scid/IL-2Rγ null mice generate a faster and more efficient disease compared to other NOD/scid-related strains. *International journal of cancer*, 123(9):2222-2227.

Amatori, S., Papalini, F., Lazzarini, R., Donati, B., Bagaloni, I., Rippo, M. R., Procopio, A., Pelicci, P. G., Catalano, A., and Fanelli, M. (2009). Decitabine, differently from DNMT1 silencing, exerts its antiproliferative activity through p21 upregulation in malignant pleural mesothelioma (MPM) cells. *Lung Cancer*, 66(2):184-190.

Amatori, S., Bagaloni, I., Macedi, E., Formica, M., Giorgi, L., Fusi, V., and Fanelli, M. (2010). Malten, a new synthetic molecule showing in vitro antiproliferative activity against tumour cells and induction of complex DNA structural alterations. *British journal of cancer*, 103(2):239-248.

Amatori, S., Ambrosi, G., Fanelli, M., Formica, M., Fusi, V., Giorgi, L., Macedi, E., Micheloni, M., Paoli, P., Pontellini, R., and Rossi, P. (2012). Synthesis, basicity, structural characterization, and biochemical properties of two [(3-hydroxy-4-pyron-2-yl) methyl] amine derivatives showing antineoplastic features. *The Journal of organic chemistry*, 77(5):2207-2218.

Arber, D. A., Orazi, A., Hasserjian, R., Thiele, J., Borowitz, M. J., Le Beau, M. M., Bloomfield, C.D., Cazzola, M., and Vardiman, J. W. (2016). The 2016 revision to the World Health Organization (WHO) classification of myeloid neoplasms and acute leukemia. *Blood*, 127(20):2391-405.

Barve, A., Kumbhar, A., Bhat, M., Joshi, B., Butcher, R., Sonawane, U., and Joshi, R. (2009). Mixed-ligand copper (II) maltolate complexes: synthesis, characterization, DNA binding and cleavage, and cytotoxicity. *Inorganic chemistry*, 48(19):9120-9132.

Besnard, E., Babled, A., Lapasset, L., Milhavet, O., Parrinello, H., Dantec, C., Marin, J. M., and Lemaitre, J. M. (2012). Unraveling cell type–specific and reprogrammable human replication origin signatures associated with G-quadruplex consensus motifs. *Nature structural & molecular biology*, 19(8):837-844.

Bird, A. P. (1980). DNA methylation and the frequency of CpG in animal DNA. *Nucleic acids research*, 8(7):1499-1504.

Bird, A., Taggart, M., Frommer, M., Miller, O. J., and Macleod, D. (1985). A fraction of the mouse genome that is derived from islands of nonmethylated, CpG-rich DNA. *Cell*, 40(1):91-99.

Bird, A. P., and Wolffe, A. P. (1999). Methylation-induced repression—belts, braces, and chromatin. *Cell*, 99(5):451-454.

Burge, S., Parkinson, G. N., Hazel, P., Todd, A. K., and Neidle, S. (2006). Quadruplex DNA: sequence, topology and structure. *Nucleic acids research*, 34(19):5402-5415.

Burnett, A. K. (2012). Treatment of acute myeloid leukemia: are we making progress? *ASH Education Program*, 2012(1):1-6.

Cavalieri, L. F. (1947). The Chemistry of the Monocyclic α-and γ-Pyrones. *Chemical reviews*, 41(3):525-584.

Cayrou, C., Coulombe, P., Puy, A., Rialle, S., Kaplan, N., Segal, E., and Méchali, M. (2012). New insights into replication origin characteristics in metazoans. *Cell Cycle*, 11(4):658-667.

Cheung, V. G., Morley, M., Aguilar, F., Massimi, A., Kucherlapati, R., and Childs, G. (1999). Making and reading microarrays. *Nature genetics*, 21:15-19.

Cline, M. J. (1994). The molecular basis of leukemia. *New England Journal of Medicine*, 330(5):328-336.

Colotta, F., Allavena, P., Sica, A., Garlanda, C., and Mantovani, A. (2009). Cancer-related inflammation, the seventh hallmark of cancer: links to genetic instability. *Carcinogenesis*, 30(7):1073-1081.

David-Cordonnier, M. H., Laine, W., Lansiaux, A., Kouach, M., Briand, G., Pierré, A., Hickman, J. A., and Bailly, C. (2002). Alkylation of guanine in DNA by S23906-1, a novel potent antitumor compound derived from the plant alkaloid acronycine. *Biochemistry*, 41(31):9911-9920.

Duggan, D. J., Bittner, M., Chen, Y., Meltzer, P., and Trent, J. M. (1999). Expression profiling using cDNA microarrays. *Nature genetics*, 21:10-14.

Elliott, W. H., and Elliott, D. C. (2009). Biochemistry and molecular biology, 4th edition. *Oxford University Press.*

Esteller, M. (2008). Epigenetics in cancer. *New England Journal of Medicine*, 358(11):1148-1159.

Fanelli, M., Caprodossi, S., Ricci-Vitiani, L., Porcellini, A., Tomassoni-Ardori, F., Amatori, S., Andreoni, F., Magnani, M., De Maria, R., Santoni, A., Minucci, S., and Pelicci, P. G. (2008). Loss of pericentromeric DNA methylation pattern in human glioblastoma is associated with altered DNA methyltransferases expression and involves the stem cell compartment. *Oncogene*, 27(3):358-365.

Fanelli, M., and Fusi, V. (2010) PCT Int. Appl. WO 2010061282 A1 20100603.

Fanelli, M., Formica, M., Fusi, V., Giorgi, L., Micheloni, M., and Paoli, P. (2016). New trends in platinum and palladium complexes as antineoplastic agents. *Coordination Chemistry Reviews*, 310:41-79.

Feinberg, A. P., and Tycko, B. (2004). The history of cancer epigenetics. *Nature Reviews Cancer*, 4(2):143-153.

Felsenfeld, G., and Groudine, M. (2003). Controlling the double helix. *Nature*, 421(6921):448-453.

Ferlay, J., Soerjomataram, I., Dikshit, R., Eser, S., Mathers, C., Rebelo, M., Parkin, D.M., Forman, D. and Bray, F. (2015). Cancer incidence and mortality worldwide: sources, methods and major patterns in GLOBOCAN 2012. *International journal of cancer*, 136(5):E359-E386.

Ferrara, N., Hillan, K. J., Gerber, H. P., and Novotny, W. (2004). Discovery and development of bevacizumab, an anti-VEGF antibody for treating cancer. *Nature Reviews Drug Discovery*, 3(5):391-400.

Gasche, C., Ahmad, T., Tulassay, Z., Baumgart, D. C., Bokemeyer, B., Büning, C., Howaldt, S., and Stallmach, A. (2015). Ferric maltol is effective in correcting iron deficiency anemia in patients with inflammatory bowel disease: results from a phase-3 clinical trial program. *Inflammatory bowel diseases*, 21(3):579-588.

Gonzalo, S., Jaco, I., Fraga, M. F., Chen, T., Li, E., Esteller, M., and Blasco, M. A. (2006). DNA methyltransferases control telomere length and telomere recombination in mammalian cells. *Nature Cell Biology*, 8(4):416-424.

Greer, E. L., and Shi, Y. (2012). Histone methylation: a dynamic mark in health, disease and inheritance. *Nature Reviews Genetics*, 13(5):343-357.

Grimwade, D. (2012). The changing paradigm of prognostic factors in acute myeloid leukaemia. *Best Practice & Research Clinical Haematology*, 25(4):419-425.

Guerzoni, C., Amatori, S., Giorgi, L., Manara, M. C., Landuzzi, L., Lollini, P. L., Tassoni, A., Balducci, M., Manfrini, M., Pratelli, L., Serra, M., Picci, P., Magnani, M., Fusi, V., Fanelli, M., and Scotlandi, K. (2014). An aza-macrocycle containing maltolic side-arms (maltonis) as potential drug against human pediatric sarcomas. *BMC cancer*, 14(1):1.

Hanahan, D., and Weinberg, R. A. (2000). The hallmarks of cancer. *Cell*, 100(1):57-70.

Hanahan, D., and Weinberg, R. A. (2011). Hallmarks of cancer: the next generation. *Cell*, 144(5):646-674.

Haskell, C. M. (2001). Cancer Treatment, 5th ed. *Saunders*.

He, Y. F., Li, B. Z., Li, Z., Liu, P., Wang, Y., Tang, Q., Ding, J., Jia, Y., Chen, Z., Li, L., Sun, Y., Li, X., Dai, Q., Song, C. X., Zhang, K., He, C., and Xu, G. L.(2011). Tet-mediated formation of 5-carboxylcytosine and its excision by TDG in mammalian DNA. *Science*, 333(6047):1303-1307.

Hironishi, M., Kordek, R., Yanagihara, R., and Garruto, R. M. (1996). Maltol (3-hydroxy-2-methyl-4-pyrone) toxicity in neuroblastoma cell lines and primary murine fetal hippocampal neuronal cultures. *Neurodegeneration*, 5(4):325-329.

Horn, P. J., and Peterson, C. L. (2002). Chromatin higher order folding--wrapping up transcription. *Science*, 297(5588):1824-1827.

Huang, D. W., Sherman, B. T., and Lempicki, R. A. (2009). Systematic and integrative analysis of large gene lists using DAVID bioinformatics resources. *Nature protocols*, 4(1):44-57.

Huang, H., Sabari, B. R., Garcia, B. A., Allis, C. D., and Zhao, Y. (2014). SnapShot: histone modifications. *Cell*, 159(2):458.

Huppert, J. L., and Balasubramanian, S. (2005). Prevalence of quadruplexes in the human genome. *Nucleic acids research*, 33(9):2908-2916.

Imamura, T., Kerjean, A., Heams, T., Kupiec, J. J., Thenevin, C., and Pàldi, A. (2005). Dynamic CpG and non-CpG methylation of the Peg1/Mest gene in the mouse oocyte and preimplantation embryo. *Journal of Biological Chemistry*, 280(20):20171-20175.

Ito, S., Shen, L., Dai, Q., Wu, S. C., Collins, L. B., Swenberg, J. A., He, C., and Zhang, Y. (2011). Tet proteins can convert 5-methylcytosine to 5-formylcytosine and 5-carboxylcytosine. *Science*, 333(6047):1300-1303.

Jakupec, M. A., and Keppler, B. K. (2004). Gallium in cancer treatment. *Current Topics in Medicinal Chemistry*, 4(15):1575-1583.

Kacem, S., and Feil, R. (2009). Chromatin mechanisms in genomic imprinting. *Mammalian Genome*, 20(9-10):544-556.

Kandioller, W., Hartinger, C. G., Nazarov, A. A., Bartel, C., Skocic, M., Jakupec, M. A., Vladimir, B. A., and Keppler, B. K. (2009). Maltol-Derived Ruthenium-Cymene Complexes with Tumor Inhibiting Properties: The Impact of Ligand-Metal Bond Stability on Anticancer Activity In Vitro. *Chemistry - A European Journal*, 15(45):12283-12291.

Kass, S. U., Pruss, D., and Wolffe, A. P. (1997). How does DNA methylation repress transcription? *Trends in Genetics*, 13(11):444-449.

Larkin, J., Goh, X. Y., Vetter, M., Pickering, L., and Swanton, C. (2012). Epigenetic regulation in RCC: opportunities for therapeutic intervention? *Nature Reviews Urology*, 9(3):147-155.

Lehnertz, B., Ueda, Y., Derijck, A. A., Braunschweig, U., Perez-Burgos, L., Kubicek, S., Chen, T., Li, E., Jenuwein, T., and Peters, A. H. (2003). Suv39h-mediated histone H3 lysine 9 methylation directs DNA methylation to major satellite repeats at pericentric heterochromatin. *Current Biology*, 13(14):1192-1200.

Li, B., Carey, M., and Workman, J. L. (2007). The role of chromatin during transcription. *Cell*, 128(4):707-719.

Li, F., Zhao, C., and Wang, L. (2014). Molecular-targeted agents combination therapy for cancer: Developments and potentials. *International Journal of Cancer*, 134(6):1257-1269.

Lister, R., Pelizzola, M., Dowen, R. H., Hawkins, R. D., Hon, G., Tonti-Filippini, J., Nery, J. R., Lee, L., Ye, Z., Ngo, Q. M., Edsall, L., Antosiewicz-Bourget, J., Stewart, R., Ruotti, V., Millar, A. H., Thomson, J. A., Ren, B., and Ecker, J. R. (2009). Human DNA methylomes at base resolution show widespread epigenomic differences. *Nature*, 462(7271):315-322.

Lopez-Serra, L., and Esteller, M. (2008). Proteins that bind methylated DNA and human cancer: reading the wrong words. *British journal of cancer*, 98(12):1881-1885.

Maizels, N., and Gray, L. T. (2013). The G4 genome. *PLoS Genetics*, *9*(4): e1003468.

Majocchi, S., Aritonovska, E., and Mermod, N. (2014). Epigenetic regulatory elements associate with specific histone modifications to prevent silencing of telomeric genes. *Nucleic acids research*, 42(1):193-204.

Mayer, W., Niveleau, A., Walter, J., Fundele, R., and Haaf, T. (2000). Embryogenesis: demethylation of the zygotic paternal genome. *Nature*, 403(6769):501-502.

Monks, A., Scudiero, D., Skehan, P., Shoemaker, R., Paull, K., Vistica, D., Hose, C., Langley, J., Cronise, P., Vaigro-Wolff, A., Gray-Goodrich, M., Campbell, H., Mayo, J., and Boyd, M. (1991). Feasibility of a high-flux anticancer drug screen using a diverse panel of cultured human tumor cell lines. *Journal of the National Cancer Institute*, 83(11):757-766.

Murakami, K., Ishida, K., Watakabe, K., Tsubouchi, R., Haneda, M., and Yoshino, M. (2006). Prooxidant action of maltol: role of transition metals in the generation of reactive oxygen species and enhanced formation of 8-hydroxy-2′-deoxyguanosine formation in DNA. *Biometals,* 19(3):253-257.

Negrini, S., Gorgoulis, V. G., and Halazonetis, T. D. (2010). Genomic instability - an evolving hallmark of cancer. *Nature Reviews Molecular Cell Biology,* 11(3):220-228.

Nováková, O., Nazarov, A. A., Hartinger, C. G., Keppler, B. K., and Brabec, V. (2009). DNA interactions of dinuclear Ru^{II} arene antitumor complexes in cell-free media. *Biochemical pharmacology,* 77(3):364-374.

Patel, J. P., Gönen, M., Figueroa, M. E., Fernandez, H., Sun, Z., Racevskis, J., Van Vlierberghe, P., Dolgalev, I., Thomas, S., Aminova, O., Huberman, K., Cheng, A., Vance, G., Higgins, R. R., Ketterling, R. P., Gallagher, R. E., Litzow, M., van den Brink, M. R. M., Lazarus, H. M., Rowe, J. M., Luger, S., Ferrando, A., Paietta, E., Tallman, M. S., Melnick, A., Abdel-Wahab, O., and Levine, R. L. (2012). Prognostic relevance of integrated genetic profiling in acute myeloid leukemia. *New England Journal of Medicine,* 366(12):1079-1089.

Pavet, V., Portal, M. M., Moulin, J. C., Herbrecht, R., and Gronemeyer, H. (2011). Towards novel paradigms for cancer therapy. *Oncogene,* 30(1):1-20.

Pereira, T. N., Webb, R. I., Reilly, P. E., Seawright, A. A., and Prakash, A. S. (1998). Dehydromonocrotaline generates sequence-selective N-7 guanine alkylation and heat and alkali stable multiple fragment DNA crosslinks. *Nucleic acids research*, 26(23):5441-5447.

Rhodes, D., and Lipps, H. J. (2015). G-quadruplexes and their regulatory roles in biology. *Nucleic acids research*, 43(18):8627-8637.

Rodriguez, R., Miller, K. M., Forment, J. V., Bradshaw, C. R., Nikan, M., Britton, S., Oelschlaegel, T., Xhemalce, B., Balasubramanian, S., and Jackson, S. P. (2012). Small-molecule–induced DNA damage identifies alternative DNA structures in human genes. *Nature chemical biology*, 8(3):301-310.

Saatchi, K., Thompson, K. H., Patrick, B. O., Pink, M., Yuen, V. G., McNeill, J. H., and Orvig, C. (2005). Coordination chemistry and insulin-enhancing behavior of vanadium complexes with maltol $C_6H_6O_3$ structural isomers. *Inorganic chemistry*, 44(8):2689-2697.

Santos, M. A. (2002). Hydroxypyridinone complexes with aluminium. In vitro/vivo studies and perspectives. *Coordination Chemistry Reviews*, 228(2):187-203.

Saxonov, S., Berg, P., and Brutlag, D. L. (2006). A genome-wide analysis of CpG dinucleotides in the human genome distinguishes two distinct classes of promoters. *Proceedings of the National Academy of Sciences*, 103(5):1412-1417.

Siddik, Z. H. (2003). Cisplatin: mode of cytotoxic action and molecular basis of resistance. *Oncogene*, 22(47):7265-7279.

Smith, Z. D., and Meissner, A. (2013). DNA methylation: roles in mammalian development. *Nature Reviews Genetics*, 14(3):204-220.

Solomon, M. J., and Varshavsky, A. (1985). Formaldehyde-mediated DNA-protein crosslinking: a probe for in vivo chromatin structures. *Proceedings of the National Academy of Sciences*, 82(19):6470-6474.

Stallmach, A., and Büning, C. (2015). Ferric maltol (ST10): a novel oral iron supplement for the treatment of iron deficiency anemia in inflammatory bowel disease. *Expert opinion on pharmacotherapy*, 16(18):2859-2867.

Stewart, B., and Wild, C. P. (2016). World cancer report 2014. *World Health Organization.*

Strahl, B. D., and Allis, C. D. (2000). The language of covalent histone modifications. *Nature*, 403(6765):41-45.

Swerdllow, S. H., Campo, E., and Harris, N. L. (2008). WHO classification of tumours of haematopoietic and lymphoid tissues. *IARC Press*.

Tennant, D. A., Durán, R. V., and Gottlieb, E. (2010). Targeting metabolic transformation for cancer therapy. *Nature Reviews Cancer*, 10(4):267-277.

The Cancer Genome Atlas Research Network. (2013). Genomic and epigenomic landscapes of adult de novo acute myeloid leukemia. *New England Journal of Medicine*, 2013(368):2059-2074.

Thompson, K. H., and Orvig, C. (2003). Boon and bane of metal ions in medicine. *Science*, 300(5621):936-939.

Thompson, K. H., Barta, C. A., and Orvig, C. (2006). Metal complexes of maltol and close analogues in medicinal inorganic chemistry. *Chemical Society Reviews*, 35(6):545-556.

Tobias, J., and Hochhauser, D. (2010). Cancer and its management, 6th edition. *Wiley-Blackwell.*

Todd, A. K., Johnston, M., and Neidle, S. (2005). Highly prevalent putative quadruplex sequence motifs in human DNA. *Nucleic acids research*, 33(9):2901-2907.

Tomizawa, S. I., Kobayashi, H., Watanabe, T., Andrews, S., Hata, K., Kelsey, G., and Sasaki, H. (2011). Dynamic stage-specific changes in imprinted differentially methylated regions during early mammalian development and prevalence of non-CpG methylation in oocytes. *Development*, 138(5):811-820.

Valton, A. L., Hassan-Zadeh, V., Lema, I., Boggetto, N., Alberti, P., Saintomé, C., Riou, J. F and Prioleau, M. N. (2014). G4 motifs affect origin positioning and efficiency in two vertebrate replicators. *The EMBO journal*, 33(7):732-746.

Verma, A., Halder, K., Halder, R., Yadav, V. K., Rawal, P., Thakur, R. K., Mohd, F., Sharma, A., and Chowdhury, S. (2008). Genome-wide computational and expression analyses reveal G-quadruplex DNA motifs as conserved cis-regulatory elements in human and related species. *Journal of medicinal chemistry*, 51(18):5641-5649.

Weinberg, R. (2014). The biology of cancer, 2nd edition. *Garland Science*.

Williamson, J. R. (1994). G-quartet structures in telomeric DNA. *Annual review of biophysics and biomolecular structure*, 23(1):703-730.

Yasumoto , E., Nakano, K., Nakayachi, T., Morshed, S. R. M., Hashimoto, K., Kikuchi, H., Nishikawa, H., Kawase, M., and Sakagami, H. (2004). Cytotoxic activity of deferiprone, maltol and related hydroxyketones against human tumor cell lines. *Anticancer research*, 24(2B):755-762.